



12-2001

A trajectory optimization and rendezvous study of a manned Mars ascent vehicle

Stephen Edward Stasko

Follow this and additional works at: https://trace.tennessee.edu/utk_gradthes

Recommended Citation

Stasko, Stephen Edward, "A trajectory optimization and rendezvous study of a manned Mars ascent vehicle. " Master's Thesis, University of Tennessee, 2001.
https://trace.tennessee.edu/utk_gradthes/9733

This Thesis is brought to you for free and open access by the Graduate School at TRACE: Tennessee Research and Creative Exchange. It has been accepted for inclusion in Masters Theses by an authorized administrator of TRACE: Tennessee Research and Creative Exchange. For more information, please contact trace@utk.edu.

To the Graduate Council:

I am submitting herewith a thesis written by Stephen Edward Stasko entitled "A trajectory optimization and rendezvous study of a manned Mars ascent vehicle." I have examined the final electronic copy of this thesis for form and content and recommend that it be accepted in partial fulfillment of the requirements for the degree of Master of Science, with a major in Aerospace Engineering.

Gary Flandro, Major Professor

We have read this thesis and recommend its acceptance:

Frank Collins, Roy Schulz

Accepted for the Council:

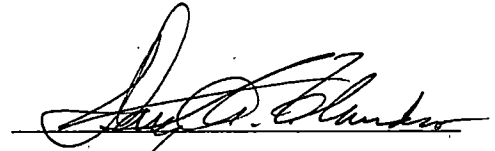
Carolyn R. Hodges

Vice Provost and Dean of the Graduate School

(Original signatures are on file with official student records.)

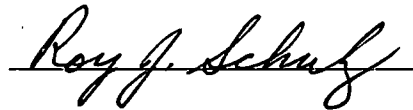
To the Graduate Council:

I am submitting herewith a thesis written by Stephen Edward Stasko entitled "A Trajectory Optimization and Rendezvous Study of a Manned Mars Ascent Vehicle." I have examined the final paper copy of this thesis for form and content and recommend that it be accepted for partial fulfillment of the requirements for the degree of Master of Science, with a major in Aerospace Engineering.

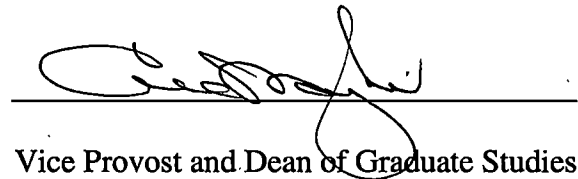


Dr. Gary Flandro, Major Professor

We have read this thesis
and recommend its acceptance:



Accepted for the Council:



Vice Provost and Dean of Graduate Studies

**A TRAJECTORY OPTIMIZATION AND
RENDEZVOUS STUDY OF A MANNED
MARS ASCENT VEHICLE**

**A Thesis
Presented for the
Master of Science
Degree
The University of Tennessee, Knoxville**

**Stephen Edward Stasko
December 2001**

DEDICATION

This thesis is dedicated to my godson:

Lawrence William Johnston III

May the things described herein
come to pass in his lifetime.

ACKNOWLEDGMENTS

I would like to thank my advisor, Dr. Gary Flandro, for the guidance and encouragement he provided throughout my graduate education at UTSI. I am fortunate to have had the opportunity to learn from such an insightful and inspiring teacher. I would like also to extend my appreciation to the other members of my committee, Dr. Frank Collins and Dr. Roy Schulz, whose suggestions helped greatly in the preparation of this thesis. I would also like to express my gratitude for all the love and support I received from my family and friends, without which I would not be where I am today.

ABSTRACT

The purpose of this study is to describe the ascent flight dynamics and orbital maneuvering requirements of a manned Mars Ascent Vehicle (MAV) within the mission structure defined by the NASA Design Reference Mission (DRM). The primary task of the MAV is to transport the astronauts and their scientific cargo from the surface of Mars to an orbiting Earth Return Vehicle (ERV), in which the crew will depart Mars orbit and begin their return to Earth. This objective comprises two phases of operation, an ascent from the Martian surface to a parking orbit, and an orbital rendezvous with the waiting ERV, and is critical to the success of a manned Mars mission.

In order to accomplish this study two programs were written to model each of the distinct phases of MAV operation. The ascent program uses Pontryagin's Maximum Principle to optimize the ascent trajectory and reduce it to a two point boundary value problem. This is then solved by the numerical method of Runge-Kutta integration, with Newton's Method used to guess the unknown initial conditions of the trajectory. This program finds the optimal trajectory to place the MAV into a parking orbit prior to rendezvous with the ERV, minimizing propellant expended and maximizing useful spacecraft payload.

The orbital rendezvous portion of the study involves quantifying the impulsive maneuvers needed to alter the MAV orbit to match its position and velocity with the ERV. This is accomplished through a study of the differential equations of relative position and velocity between the two vehicles. The resulting boundary value problem is

solved using the numerical methods of Runge-Kutta integration and Newton's Method, providing the necessary maneuvers to achieve orbital rendezvous.

TABLE OF CONTENTS

CHAPTER	PAGE
1. INTRODUCTION	1
2. ASCENT ANALYSIS	4
2.1 History of Trajectory Optimization	4
2.2 Pontryagin Maximum Principle	6
2.3 Equations of Motion for an Ascending Spacecraft	8
2.4 Trajectory Optimization	14
2.5 Ascent Calculation Results	19
2.5.1 Powered All the Way Ascent	21
2.5.2 Coast to Orbit Ascent	24
2.5.3 Low Orbit with Hohmann Transfer Ascent	31
3. RENDEZVOUS ANALYSIS	36
3.1 Equations of Relative Motion	36
3.2 Solution Method	40
3.3 Rendezvous Calculation Results	42
3.3.1 Non Co-orbital Rendezvous Case	44
3.3.2 Co-orbital Rendezvous Case	47
4. CONCLUSIONS	50
5. RECOMMENDATIONS FOR FURTHER STUDY	53
LIST OF REFERENCES	54
APPENDICES	58
APPENDIX A: ASCENT OPTIMIZATION CODE	59

APPENDIX B: RENDEZVOUS CODE

67

VITA

75

LIST OF TABLES

TABLE		PAGE
Table 2.4.1	Boundary Value Conditions for Ascent Trajectory Optimization	19
Table 3.2.1	Boundary Value Conditions for Rendezvous Problem	41
Table 4.1	Summary of Launch Strategy Performance	50
Table 4.2	Summary of Acceleration and Control Angle Characteristics	51
Table 4.3	Summary of Rendezvous Performance	52

LIST OF FIGURES

FIGURE		PAGE
Figure 2.3.1	Free Body Diagram of an Ascending Spacecraft	9
Figure 2.5.1	Trajectory for PAW Ascent	22
Figure 2.5.2	Control Angle History for PAW Ascent	23
Figure 2.5.3	Periapsis Altitude of Coast Orbit vs. Circularization ΔV	26
Figure 2.5.4	ΔV Remaining vs. Engine Cutoff Altitude for Coast to Orbit Ascent	27
Figure 2.5.5	Trajectory for Coast to Orbit Ascent	29
Figure 2.5.6	Control Angle History for Coast to Orbit Ascent	30
Figure 2.5.7	Trajectory for Ascent to Low Orbit with Hohmann Transfer	33
Figure 2.5.8	Control Angle History for Ascent to Low Orbit with Hohmann Transfer	34
Figure 3.1.1	Coordinate System for Rendezvous	37
Figure 3.3.1	ΔV vs. Time for Non Co-orbital Rendezvous with ERV 62.13 km ahead of MAV	45
Figure 3.3.2	ΔV vs. Time for Non Co-orbital Rendezvous with ERV 62.13 km behind MAV	46
Figure 3.3.3	ΔV vs. Time for Co-orbital Rendezvous with ERV 62.13 km ahead of MAV	48
Figure 3.3.4	ΔV vs. Time for Co-orbital Rendezvous with ERV 62.13 km behind MAV	49

LIST OF SYMBOLS AND ACRONYMS

a	Semimajor axis
C	Kepler area constant
DRM	Design reference mission
e	Eccentricity
ERV	Earth return vehicle
F	Thrust force
F_x	Thrust force in the x direction of the ERV body centered coordinates
F_y	Thrust force in the y direction of the ERV body centered coordinates
F_z	Thrust force in the z direction of the ERV body centered coordinates
g_e	Gravitational acceleration on the surface of Earth, 9.811 m/s
g_m	Gravitational acceleration on the surface of Mars, 3.909 m/s
g_x	Gravitational acceleration in the x direction of the ERV body centered coordinates
g_y	Gravitational acceleration in the y direction of the ERV body centered coordinates
g_z	Gravitational acceleration in the z direction of the ERV body centered coordinates
g_T	Gravitational acceleration of the target vehicle during rendezvous
GM	Mars gravitational constant, $4.28283 \times 10^{13} \text{ m}^3/\text{s}^2$
H	Hamiltonian
h	Orbital energy Constant
ISP	Specific impulse

ISPP	In-situ propellant production
m_0	Initial mass of the spacecraft
m_f	Mass of fuel
m_{pl}	Mass of payload
m_s	Mass of spacecraft structure
\dot{m}	Mass flow rate of the spacecraft rocket engine
MAV	Mars Ascent Vehicle
NASA	National Aeronautics and Space Administration
PAW	Powered-all-the-way
PMP	Pontryagin Maximum Principle
Q	Generalized force or moment in Lagrange equation
Q_r	Generalized force in the radial direction
Q_θ	Generalized moment in the tangential direction
r	Radial position of the spacecraft, measured from planet's surface
r_{cut}	radial position at engine cutoff
r_T	Radial position of the target spacecraft in rendezvous calculations
$r_{250\text{ km}}$	Radius of a 250 km altitude circular orbit, 3560 km
R_p	Mean radius of Mars, 3310 km
t	Time
T	Kinetic energy
v	Spacecraft velocity
v_{cut}	Spacecraft velocity at engine cutoff
v_r	Radial component of spacecraft velocity

v_{θ}	Tangential component of spacecraft velocity
z_r	costate variable corresponding to radial position
z_{vr}	costate variable corresponding to radial velocity
$z_{v\theta}$	costate variable corresponding to tangential position
α	Control angle of engine gimbal or spacecraft steering
γ	Angle of flight path to local horizontal
ρ	Position of the MAV with respect to position of the ERV
ρ_x	X direction position of the MAV with respect to the ERV body centered coordinate system
ρ_y	Y direction position of the MAV with respect to the ERV body centered coordinate system
ρ_z	Z direction position of the MAV with respect to the ERV body centered coordinate system
θ	Angular position of spacecraft measured from launch site

1. INTRODUCTION

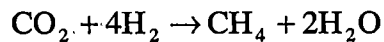
Among the long term plans of the National Aeronautics and Space Administration is a manned mission to Mars, which it is hoped may occur within the first half of this century. The requirements for such an imposing goal are being tentatively explored in NASA's Design Reference Mission, an evolving mission strategy that is periodically updated to include current and proposed technological advances.

While the problems of sending humans to the nearest planet are daunting, the provision for their safe return is an equally intimidating task. NASA's current mission strategy attempts to alleviate these challenges through the pre-positioning of redundant pieces of equipment for use in each phase of the mission architecture. When the first crew arrives on Mars, a waiting MAV will have already been there almost two years. Shortly after their arrival on Mars surface a second MAV, originally intended for use by the second visiting crew, will arrive, providing a backup ability for the crew to reach orbit should the first vehicle prove inoperable.

The ascent from the Martian surface and subsequent rendezvous with the Earth Return Vehicle is budgeted with the single largest ΔV of any maneuver in the mission, approximately 5.6 kilometers per second [1]. The MAV has been designed to carry 39,000 kg of propellant to achieve the combined ascent and rendezvous with the ERV. The MAV itself consists of an a crew capsule weighing 4829 kg, an empty propulsion module mass of 4069 kg, and a payload consisting of four crew members and scientific equipment weighing approximately 1000 kg. MAV propulsion is supplied by four RL-10

class engines modified to burn a mix of oxygen and methane and operating with an average specific impulse of 379 seconds [2].

Significant savings in mission mass are achieved by producing the propellant needed by the MAV on the surface of Mars, using in-situ propellant production. Carbon dioxide from the Martian atmosphere is combined with a supply of pre-delivered hydrogen feedstock to produce methane and water through the Sabatier reaction [3]. This chemical reaction functions without input of any energy in the presence of a nickel catalyst by the following chemical formula:



Despite the savings made in overall mission mass through the use of in-situ propellant production (ISPP) technology, it is still desirable to be able to launch the MAV from the surface of the planet to its rendezvous with the ERV using a minimum of fuel, maximizing the mass of the vehicle dedicated to the astronauts and their scientific cargo and minimizing the portion of the vehicle mass dedicated to propellant systems.

Once in orbit the crew will then rendezvous and transfer to the Earth Return Vehicle in which they will leave Mars orbit and return home. The ERV has been aerobraked into a highly elliptical orbit around Mars, with a periapsis altitude of 250 km and an apoapsis altitude of 33793 km [4]. The high eccentricity of this orbit, 0.8249, leads to the need to perform rendezvous with the ERV near the periapsis position of its orbit. This requires careful timing of the MAV launch from the surface to place it in the vicinity of the ERV as it comes sailing by at the low point of its orbit. The maneuvers needed to accomplish rendezvous are then specified through the equations of relative

motion between the two spacecraft, with a desired final relative position of zero distance and zero relative velocity between the two spacecraft.

2. ASCENT ANALYSIS

2.1 History of Trajectory Optimization.

The problem of trajectory optimization was dealt with from the beginning uses of the guided missile as a weapon of war. The first numerical solutions to the problem of powered ascent grew out of the V-2 rocket program undertaken by the German's during World War II. As the ranges of early guided missiles were relatively small, these calculations were in a Cartesian format with corrections for the earth's curvature inserted into longer range trajectories.

These earliest methods of range optimization involved establishing the vehicle in a predetermined position and velocity at the end of its vertical climb. These predetermined flight conditions at the end of the climb formed the initial values to be inserted into the non-controlled ballistic equations of motion for the vehicle. This method therefore is not a continuously controlled system, as control forces were exerted on the vehicle only at the end point of the vertical climb.

A graphical method, in which the vectors of the change of velocity caused by vehicle thrust, aerodynamic forces, and gravitational losses, can be used to determine the optimum continuously controlled pitch program for an ascending space vehicle. Such a method can be easily used to determine a controlled trajectory for a vehicle ascending into orbit, but this analysis is again performed in Cartesian format, necessitating the addition of correction factors for the curvature of the earth. This method grew out of the V-2 program and remained in use in missile range calculations during the 1950's [5].

An analytic solution can be found to the optimal ascent problem if several assumptions are made. The first of these assumptions states that the thrust of the ascending vehicle, and thus its mass flow rate, must be constant. The second assumption states that the gravity acting on the vehicle is a linear function of its radial position. These assumptions reduce the representation of the problem to that of a harmonic oscillator with a forcing function. A solution can therefore be found through the method of variation of parameters [6].

A solution to a continuous controlled trajectory problem can be sought through the method of calculus of variations. In this approach a particular performance index of a vehicle is minimized by enforcing the Euler Lagrange condition. This generally reduces the trajectory problem to a two point boundary value problem, which can be solved by several numerical techniques, including steepest ascent and the Newton-Raphson method [7].

The Euler Lagrange condition that is the basis of the calculus of variations approach to the problem becomes inconvenient as the number of parameters in the problem increase. The cases when these equations can be integrated in closed form are limited [8]. An alternative to the calculus of variations method lies in the study of the Hamiltonian of a dynamic system. Hamiltonian-based optimization techniques, an example of which is the Pontryagin Maximum Principle used in this study, have been utilized for trajectory calculations on the upper stages of Saturn boosters in the 1960's [9].

2.2 Pontryagin Maximum Principle

Considering a problem with an n -dimensional state vector x and state equations defined as

$$\dot{x}_i = f_i(x, u) \quad i = 1, 2, \dots, n$$

where u is a control vector. A transfer is sought from an initial state x^0 at time zero to a final desired state x^f at some unspecified time t_f . There exists a control as a function of time, $u(t)$, that will accomplish this transfer while minimizing a cost function

$$J = \int_{t_0}^{t_f} f_0(x, u) dt$$

where $f_0(x, u)$ is a state equation corresponding to an additional state variable x_0 ,

$$\dot{x}_0 = f(x, u)$$

Added to the previous state vector x this additional state variable forms the state vector \hat{x} with dimension $n+1$ and corresponding state equations

$$\dot{\hat{x}}_i = \hat{f}_i(x, u) \quad i = 0, 1, 2, \dots, n$$

From the extended state vector the Hamiltonian of the system, a function of the state variable, the costate variable, and the control, can be defined as

$$H = \hat{z}^T \dot{\hat{x}} = \sum_{i=0}^n z_i f_i \quad i = 0, 1, 2, \dots, n$$

where \hat{z} represents an extended co-state vector with $n+1$ dimensions. The equations for both the state and costate vector can be defined by the following equations:

$$\frac{dx_i}{dt} = \frac{\partial H}{\partial z_i} \quad i = 1, 2, \dots, n$$

$$\frac{dz_i}{dt} = -\frac{\partial H}{\partial x_i} \quad i = 1, 2, \dots, n$$

Since the value of the Hamiltonian does not depend on the additional state variable x_0 , the equation for its corresponding costate variable is

$$\dot{z}_0 = 0$$

Having stated the problem in terms of its Hamiltonian, with accompanying state and costate variables, the PMP can be applied to the problem. The four basic conditions of the PMP are as follows [10]:

1. The Pontryagin maximum principle states that an arbitrary value of negative one is assigned to z_0 . This leads to the modified expression of the Hamiltonian:

$$H = -f_0 + \sum_{i=1}^n z_i f_i \quad i = 1, 2, \dots, n$$

2. The optimum control function, according to the Pontryagin maximum principle, will maximize the Hamiltonian to a value greater than or equal to zero for all time during an optimal trajectory. The equation for the optimum control function is obtained using the following equation:

$$\frac{\partial H}{\partial u} = 0$$

3. There exists a set of initial values for the costate vector and state vector that will transfer the values of the state vector from their initial state to a desired final state.
4. Along an optimal trajectory the Hamiltonian exhibits a constant value. This constant value is positive if the final time is fixed and is zero if the final time is free.

The problem as stated now has a set of $2n + 2$ state and costate equations. These equations are solved by the n known initial and final values, the initial value of x_0 , and the value of z_0 . For final time free problems, such as the one in this study, the unknown final time requires an additional known final condition. This condition is supplied by the fourth statement of the PMP.

2.3 Equations of Motion for an Ascending Spacecraft

The equations of motion for a powered ascent vehicle can be derived by the use of Lagrange's equation for non-conservative forces:

$$\frac{d}{dt} \left(\frac{\partial T}{\partial \dot{q}} \right) - \frac{\partial T}{\partial q} = Q_i$$

where T is the kinetic energy of the spacecraft, q is an appropriate set of generalized coordinates and Q_i is the generalized force on the spacecraft. The equations of motion for this problem will be derived for polar coordinates with the origin located at the center of the planet to eliminate any correcting terms for trajectory curvature that are inherent to rectangular derivation of the equations [11]. Expressing the equations of motion in polar coordinates is also beneficial in that they can be viewed as the equations of orbital motion with the addition of a thrusting force. The coordinate system and a free body diagram of the forces on the vehicle are illustrated in figure 2.3.1.

The generalized coordinates for the problem are radial and angular position of the spacecraft with respect to the center of Mars. For this study it is assumed that the thrust vector always passes through the vehicle's center of gravity. For a vehicle with a gimbaling engine, this assumes that the pitching moments produced by the

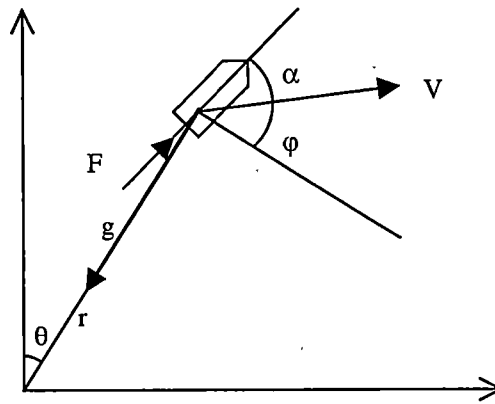


Figure 2.3.1: Free Body Diagram of an Ascending Spacecraft

gimballed engine are small. This simplification does not lead to large inaccuracies in the calculations, as current designs for the MAV have a wide squat appearance, with the center of mass riding low in the vehicle near the engines. For a vehicle without engine-gimballing ability, this assumption is accurate, as steering changes are made by maneuvering the entire vehicle at a desired angle to its velocity vector. This study also neglects the aerodynamic effects of lift and drag on the vehicle as it ascends through the atmosphere. Atmospheric drag has minimal effects on the trajectory of an ascending spacecraft in Earth's atmosphere. The low density of Mars' atmosphere will lead to lower dynamic pressures than experienced in Earth's atmosphere, producing an even smaller drag on the MAV.

The first step in using Lagrange's equations is to express the kinetic energy of the spacecraft as:

$$T = \frac{1}{2} m (\dot{r}^2 + (r\dot{\theta})^2)$$

Lagrange's equation for the first generalized coordinate, radial position, is:

$$\frac{d}{dt} \left(\frac{\partial T}{\partial \dot{r}} \right) - \frac{\partial T}{\partial r} = Q_r$$

The generalized force in the radial direction is made up of the radial components of gravity and engine thrust and is expressed as:

$$Q_r = m \left(-\frac{GM}{r^2} + \frac{F}{m} \sin(\varphi + \alpha) \right)$$

The partial derivatives of the kinetic energy expression with respect to radial position and time rate of change of radial position are:

$$\frac{\partial T}{\partial \dot{r}} = m\dot{r}$$

$$\frac{\partial T}{\partial r} = m r \dot{\theta}^2$$

The above equations are inserted into Lagrange's equation and the common mass variable present in each term can be divided out, producing the following expression:

$$\ddot{r} - r\dot{\theta}^2 = -\frac{GM}{r^2} + \frac{F}{m} \sin(\varphi + \alpha)$$

Since the radial component of velocity is the product of the radius and the angular rate of change the differential equation for the radial rate of change can be expressed as:

$$\frac{dv_r}{dt} = \frac{v_\theta^2}{r} - \frac{GM}{r^2} + \frac{F}{m} \sin(\varphi + \alpha)$$

Lagrange's equation for the second of the two generalized coordinates, angular position, is:

$$\frac{d}{dt} \left(\frac{\partial T}{\partial \dot{\theta}} \right) - \frac{\partial T}{\partial \theta} = Q_\theta$$

The generalized torque in the angular direction is made up only of the angular component of engine thrust, since gravity is only active in the radial direction and is expressed as:

$$Q_{\theta} = F \cdot \cos(\varphi + \alpha) \cdot r$$

The partial derivatives of the kinetic energy with respect to angular position and time rate of change of angular position are:

$$\frac{\partial T}{\partial \dot{\theta}} = mr^2 \dot{\theta}$$

$$\frac{\partial T}{\partial \theta} = 0$$

By again noting that the tangential velocity is equal to the product of the radial position and the rate of change of angular position the partial derivative of the kinetic energy with respect to rate of change of angular position can be expressed in the following form:

$$\frac{\partial T}{\partial \dot{\theta}} = mr v_{\theta}$$

The above equations are inserted into Lagrange's equation and the common mass variable present in each term can be divided out, producing the following equation:

$$\frac{d}{dt}(r v_{\theta}) = \frac{F}{m} \cdot \cos(\varphi + \alpha) \cdot r$$

By expanding the time derivative in the above equation the differential equation for the tangential velocity can be written as:

$$\frac{dv_{\theta}}{dt} = -\frac{v_r v_{\theta}}{r} + \frac{F}{m} \cos(\varphi + \alpha)$$

In order to perform Runge-Kutta integration upon the two derived equations, we must have a set of two differential equations to describe the radial and angular position, so that

the total set can be treated as four first order differential equations. This produces the set of equations as follows:

$$\frac{dr}{dt} = v_r$$

$$\frac{d\theta}{dt} = \frac{v_\theta}{r}$$

$$\frac{dv_r}{dt} = \frac{v_\theta^2}{r} - \frac{GM}{r^2} + \frac{F}{m} \sin(\varphi + \alpha)$$

$$\frac{dv_\theta}{dt} = -\frac{v_r v_\theta}{r} + \frac{F}{m} \cos(\varphi + \alpha)$$

In order to carry out a numerical solution to the problem it is useful to non-dimensionalize the equations. This would reduce the time taken for a computer to complete the numerical calculation. The non-dimensional values for velocity, length, and time can be calculated from the following equations:

$$r = \frac{r^*}{R_p}$$

$$v = \frac{v^*}{\sqrt{\frac{GM}{R_p}}}$$

$$t = \frac{t^*}{\sqrt{\frac{R_p^3}{GM}}}$$

where the asterisk superscript denotes the dimensional variable. As can be seen in the above equations, the scaling variables for radial position is the radius of Mars, R_p . The circular orbit speed at the surface of Mars is the velocity scaling variable. A time scaling

variable is derived from dividing the distance scaling variable by the velocity scaling variable. The dimensionless equations of motion for an ascending spacecraft take the form:

$$\frac{R_p}{\sqrt{\frac{R_p^3}{GM}}} \frac{dr^*}{dt^*} = v_r^* \sqrt{\frac{GM}{R_p}}$$

$$\frac{1}{\sqrt{\frac{R_p^3}{GM}}} \frac{d\theta^*}{dt^*} = \frac{v_\theta^*}{r^*} \sqrt{\frac{GM}{R_p}}$$

$$\frac{\sqrt{\frac{GM}{R_p}}}{\sqrt{\frac{R_p^3}{GM}}} \frac{dv_r^*}{dt^*} = \frac{v_\theta^{*2}}{r^*} \frac{\left(\sqrt{\frac{GM}{R_p}}\right)^2}{R_p} - \frac{GM}{r^{*2}} \frac{\sqrt{\frac{R_p^3}{GM}}}{\sqrt{\frac{GM}{R_p}}} \frac{1}{R_p^2} + \frac{F}{m} \sin(\varphi + \alpha) \frac{\sqrt{\frac{R_p^3}{GM}}}{\sqrt{\frac{GM}{R_p}}}$$

$$\frac{\sqrt{\frac{GM}{R_p}}}{\sqrt{\frac{R_p^3}{GM}}} \frac{dv_\theta^*}{dt^*} = -\frac{v_r^* v_\theta^*}{r^*} \frac{\left(\sqrt{\frac{GM}{R_p}}\right)^2}{R_p} + \frac{F}{m} \cos(\varphi + \alpha) \frac{\sqrt{\frac{R_p^3}{GM}}}{\sqrt{\frac{GM}{R_p}}}$$

Simplification of the above equations, and the dropping of the asterisk for clarity, as it is no longer needed, obtains the dimensionless state equations in their final form:

$$\frac{dr}{dt} = v_r$$

$$\frac{d\theta}{dt} = \frac{v_\theta}{r}$$

$$\frac{dv_r}{dt} = \frac{v_\theta^2}{r} - \frac{1}{r^2} + \frac{F}{mg_m} \sin(\varphi + \alpha)$$

$$\frac{dv_{\theta}}{dt} = -\frac{v_r v_{\theta}}{r} + \frac{F}{mg_m} \cos(\phi + \alpha)$$

where g_m is the gravitational acceleration on the surface of Mars. It is this set of equations to which the PMP will be applied in order to optimize the ascent trajectory for minimum fuel expenditure.

2.4 Trajectory Optimization

The first phase of the MAV mission is to ascend from the surface of Mars into an orbit suitable for rendezvous with the ERV. The problem undertaken in this study is to achieve a rendezvous orbit while burning a minimum amount of propellant. The cost function for this problem is then stated as

$$J = \int_0^{t_f} (\dot{m}) dt$$

For this study, the MAV is assumed to have a constant mass flow rate. This allows us to treat the optimization of the trajectory as a minimum time problem, simplifying the cost function to the following form:

$$J = \int_0^{t_f} 1 dt$$

The state vector of the ascent vehicle is composed of its radial and tangential components of its position and velocity, a total of four state variables. It is observed that none of the state equations are dependent on the angular position, θ , of the ascent vehicle nor is angular position a specified value in the desired final state of the system. The angular position is therefore seen to be unimportant and can be disregarded in the optimization procedure [12]. This allows the number of state equations to be reduced from four to

three. The value of the angular position of the ascending spacecraft will be of interest, however, in calculating the downrange distance covered by the MAV. The corresponding state equations are as follows:

$$f_1 = \frac{dr}{dt} = v_r$$

$$f_2 = \frac{dv_r}{dt} = \frac{v_\theta^2}{r} - \frac{1}{r^2} + \frac{F}{mg_m} \sin(\varphi + \alpha)$$

$$f_3 = \frac{dv_\theta}{dt} = -\frac{v_r v_\theta}{r} + \frac{F}{mg_m} \cos(\varphi + \alpha)$$

Optimization of the trajectory by the PMP is based upon the maximizing the Hamiltonian of the system. The Hamiltonian of the ascent vehicle can be expressed in the following equation:

$$H = -1 + z_r(v_r) + z_{v_r} \left(\frac{v_\theta^2}{r} - \frac{1}{r^2} + \frac{F}{mg_m} \sin(\varphi + \alpha) \right) + z_{v_\theta} \left(-\frac{v_r v_\theta}{r} + \frac{F}{mg_m} \cos(\varphi + \alpha) \right)$$

The set of costate differential equations are derived from the partial derivatives of the Hamiltonian with respect to each state variable and are as follows:

$$\frac{dz_r}{dt} = -\frac{\partial H}{\partial r} = z_{v_r} \left(\frac{v_\theta^2}{r^2} - \frac{2}{r^3} \right) + z_{v_\theta} \left(-\frac{v_r v_\theta}{r^2} \right)$$

$$\frac{dz_{v_r}}{dt} = -\frac{\partial H}{\partial v_r} = -z_r + z_{v_r} \left(-\frac{F}{mg_m} \frac{\partial}{\partial v_r} \sin(\varphi + \alpha) \right) + z_{v_\theta} \left(\frac{v_\theta}{r} - \frac{F}{mg_m} \frac{\partial}{\partial v_r} \cos(\varphi + \alpha) \right)$$

$$\frac{dz_{v_\theta}}{dt} = -\frac{\partial H}{\partial v_\theta} = z_{v_r} \left(-\frac{2v_\theta}{r} - \frac{F}{mg_m} \frac{\partial}{\partial v_\theta} \sin(\varphi + \alpha) \right) + z_{v_\theta} \left(\frac{v_r}{r} - \frac{F}{mg_m} \frac{\partial}{\partial v_\theta} \cos(\varphi + \alpha) \right)$$

The above equations contain derivatives of the sine and cosine of angle φ , the angle between the MAV's velocity vector and the local horizontal. This angle can be expressed in terms of the radial and tangential components of the vehicle velocity by the relation:

$$\varphi = \tan^{-1} \left(\frac{v_r}{v_\theta} \right)$$

The magnitude of the velocity vector can also be expressed in terms of the components of velocity by the following relation:

$$v = \sqrt{v_r^2 + v_\theta^2}$$

The partial derivatives of the trigonometric functions of the control angle and angle to local horizontal can be written in the following form:

$$\frac{\partial}{\partial v_r} \sin(\varphi + \alpha) = \cos(\varphi + \alpha) \frac{\partial \varphi}{\partial v_r} = \frac{v_\theta}{v^2} \cos(\varphi + \alpha)$$

$$\frac{\partial}{\partial v_r} \cos(\varphi + \alpha) = -\sin(\varphi + \alpha) \frac{\partial \varphi}{\partial v_r} = -\frac{v_\theta}{v^2} \sin(\varphi + \alpha)$$

$$\frac{\partial}{\partial v_\theta} \sin(\varphi + \alpha) = \cos(\varphi + \alpha) \frac{\partial \varphi}{\partial v_\theta} = -\frac{v_r}{v^2} \cos(\varphi + \alpha)$$

$$\frac{\partial}{\partial v_\theta} \cos(\varphi + \alpha) = -\sin(\varphi + \alpha) \frac{\partial \varphi}{\partial v_\theta} = \frac{v_r}{v^2} \sin(\varphi + \alpha)$$

The equation for the optimal control of the steering angle is found by setting the partial derivative of the Hamiltonian with respect to the control equal to zero, yielding the following expression:

$$\frac{\partial H}{\partial \alpha} = 0 = z_{v_r} \left(\frac{F}{mg_m} \frac{\partial}{\partial \alpha} \sin(\varphi + \alpha) \right) + z_{v_\theta} \left(\frac{F}{mg_m} \frac{\partial}{\partial \alpha} \cos(\varphi + \alpha) \right)$$

The partial derivatives of the sine and cosine of α , the angle between the velocity vector and the thrust vector of the MAV, are expressed by the following equations:

$$\frac{\partial}{\partial \alpha} \sin(\varphi + \alpha) = \cos(\varphi + \alpha)$$

$$\frac{\partial}{\partial \alpha} \cos(\varphi + \alpha) = -\sin(\varphi + \alpha)$$

Inserting these into the partial derivative of the Hamiltonian with respect to the control angle leads to the following expression:

$$z_{v_r} \left(\frac{F}{mg_m} \cos(\varphi + \alpha) \right) = z_{v_\theta} \left(\frac{F}{mg_m} \sin(\varphi + \alpha) \right)$$

Simplifying the above equation yields the following relation:

$$\tan(\varphi + \alpha) = \frac{z_{v_r}}{z_{v_\theta}}$$

Solving the above expression for α yields an expression for the control law of the system:

$$\alpha = \tan^{-1} \left(\frac{z_{v_r}}{z_{v_\theta}} \right) - \varphi$$

This expression for the engine control angle is inserted back into the equations of motion for the state and costate variables, resulting in the following set of six differential equations:

$$\frac{dr}{dt} = v_r$$

$$\frac{dv_r}{dt} = \frac{v_\theta^2}{r} - \frac{1}{r^2} + \frac{F}{mg_m} \sin \left(\tan^{-1} \left(\frac{z_{v_r}}{z_{v_\theta}} \right) \right)$$

$$\frac{dv_{\theta}}{dt} = -\frac{v_r v_{\theta}}{r} + \frac{F}{mg_m} \cos\left(\tan^{-1}\left(\frac{z_{v_r}}{z_{v_0}}\right)\right)$$

$$\frac{dz_r}{dt} = z_{v_r} \left(\frac{v_{\theta}^2}{r^2} - \frac{2}{r^3} \right) + z_{v_0} \left(-\frac{v_r v_{\theta}}{r^2} \right)$$

$$\frac{dz_{v_r}}{dt} = -z_r + z_{v_r} \left(-\frac{F}{mg_m} \frac{v_{\theta}}{v^2} \cos\left(\tan^{-1}\left(\frac{z_{v_r}}{z_{v_0}}\right)\right) \right) + z_{v_0} \left(\frac{v_{\theta}}{r} + \frac{F}{mg_m} \frac{v_{\theta}}{v^2} \sin\left(\tan^{-1}\left(\frac{z_{v_r}}{z_{v_0}}\right)\right) \right)$$

$$\frac{dz_{v_0}}{dt} = -\frac{\partial H}{\partial v_{\theta}} = z_{v_r} \left(-\frac{2v_{\theta}}{r} + \frac{F}{mg_m} \frac{v_r}{v^2} \cos\left(\tan^{-1}\left(\frac{z_{v_r}}{z_{v_0}}\right)\right) \right) + z_{v_0} \left(\frac{v_r}{r} - \frac{F}{mg_m} \frac{v_r}{v^2} \sin\left(\tan^{-1}\left(\frac{z_{v_r}}{z_{v_0}}\right)\right) \right)$$

This set is treated as a boundary value problem and solved by fourth order Runge-Kutta integration. In order to solve the boundary value problem the number of known final conditions must equal the number of unknown initial conditions.

A list of the known and unknown conditions in this problem appears in table 2.4.1. The three unknown initial values of the costate variables and the final time in which the ascent is performed are the four unknown initial values. The program written to solve this problem, however, analyzes the equations and provides a set of initial costate variables for each successive time step. This method eliminates time as an unknown and requires the specification of only three known final conditions. These three conditions that must be specified within the program are the final radial position, the final radial velocity, and the final value of the Hamiltonian, which is also zero, according to the PMP. An algorithm based on Newton's method will produce guesses for the values of the unknown initial conditions for the costate vector that will, when the equations are integrated over time, will generate the desired final conditions of radial position and

Table 2.4.1: Boundary Value Conditions for Ascent Trajectory Optimization

Variable	Initial Condition	Final Condition
Radial position	known	known
Radial velocity	known	known
Tangential velocity	known	known
Radial position costate	unknown	unknown
Radial velocity costate	unknown	unknown
Tangential velocity costate	unknown	unknown
Hamiltonian	known	known
Time	known	unknown

velocity and Hamiltonian. As the program converges on the zero Hamiltonian and radial position and velocity requirements, the selection of final time and its accompanying set of initial costate variables is then made by picking the time step at which the tangential velocity of the MAV is equal to the tangential velocity calculated for the desired final orbit of the vehicle.

2.5 Ascent Calculation Results

Three different ascent strategies for placing the MAV into an orbit from which it can perform a rendezvous with the ERV are analyzed in this study. The first ascent strategy is a powered-all-the-way (PAW) ascent in which the MAV is placed into a 250 km circular orbit in one continuous powered maneuver.

The second strategy examined in this study is a powered ascent to a point on an elliptical orbit with a periapsis altitude of 250 km. At a desired altitude the engines are

shutdown and the MAV will coast along this orbit to the periapsis point. At periapsis a maneuver is made to circularize the MAV orbit at 250 km altitude.

The third ascent strategy is composed of a powered ascent to a low circular orbit slightly above Mars atmosphere, at which point a two-impulse Hohmann ellipse-style maneuver is made to raise the orbit to the desired 250 km altitude.

For each strategy, the MAV is constrained to climb vertically to an altitude of 3 km before the control function is allowed to alter the MAV course. The trajectory is held vertical through the densest part of Mars' atmosphere to limit the aerodynamic side loading on the MAV in an effort to reduce its structural weight [5]. An additional assumption in this study is that the elimination of effects on the trajectory caused by the rotation of Mars.

A figure of merit used to judge each ascent strategy is the ΔV required to alter the 250 km altitude circular orbit to the highly eccentric orbit in which the ERV is waiting. This ΔV , 1217.053 m/s, is calculated by the subtraction of the MAV 250 km circular orbit velocity from the ERV periapsis velocity, according to the equation

$$\Delta V = \sqrt{\frac{GM}{r_c}(1+e)} - \sqrt{\frac{GM}{r_c}}$$

This ΔV can be used to calculate an initial estimate of the propellant required to complete the rendezvous maneuver, that is, the propellant that must remain aboard the vehicle once it has completed its ascent to the 250 km circular orbit. This mass of propellant needed for the orbital maneuvering, 3833.251 kg, is calculated by the equation:

$$m_f = (m_s + m_{pl}) \cdot \left(e^{\frac{\Delta V}{I_{sp} \cdot g_0}} - 1 \right)$$

2.5.1 Powered All the Way Ascent

The first ascent strategy involves direct ascent into the desired final orbital flight conditions in one continuous firing of the engine. The desired engine shutoff conditions of the ascent maneuver are a final altitude of 250 km, a radial velocity of 0 meters per second, and a tangential velocity equal to the circular orbit velocity at 250 km. This value is 3471.634 meters per second and is found by the formula [13]:

$$v = \sqrt{\frac{GM}{r}}$$

The PAW ascent strategy requires the engines to run for 461.5 seconds. The trajectory followed by the spacecraft for the PAW ascent is shown in figure 2.5.1. Due to the constant mass flow rate, non throttling engine assumed in this study, the highest acceleration felt on the MAV occurs at engine shutdown. This acceleration has a value of 24.13 m/s, corresponding to 2.46 Earth gravities and 6.173 Mars gravities.

A control angle history is given for the PAW ascent in figure 2.5.2. It can be observed that for the first 52.45 seconds of flight there is no control angle exerted on the vehicle trajectory. This corresponds to the vertically constrained ascent to the desired pitchover altitude of 3 km. After reaching pitchover altitude a control function generated by the PMP guides the vehicle to the desired final orbital conditions. From figure 2.5.2 it can be seen that the largest absolute value of the control angle is 42.65 degrees. This angle is too large to be achieved through a gimbaling of the engine and must be accomplished by orientating the entire vehicle at an angle to its velocity vector. This validates the assumption made in this study that the engine thrust would act through the vehicle center of gravity. At the point of engine shutdown the MAV has only 2366.16 kg

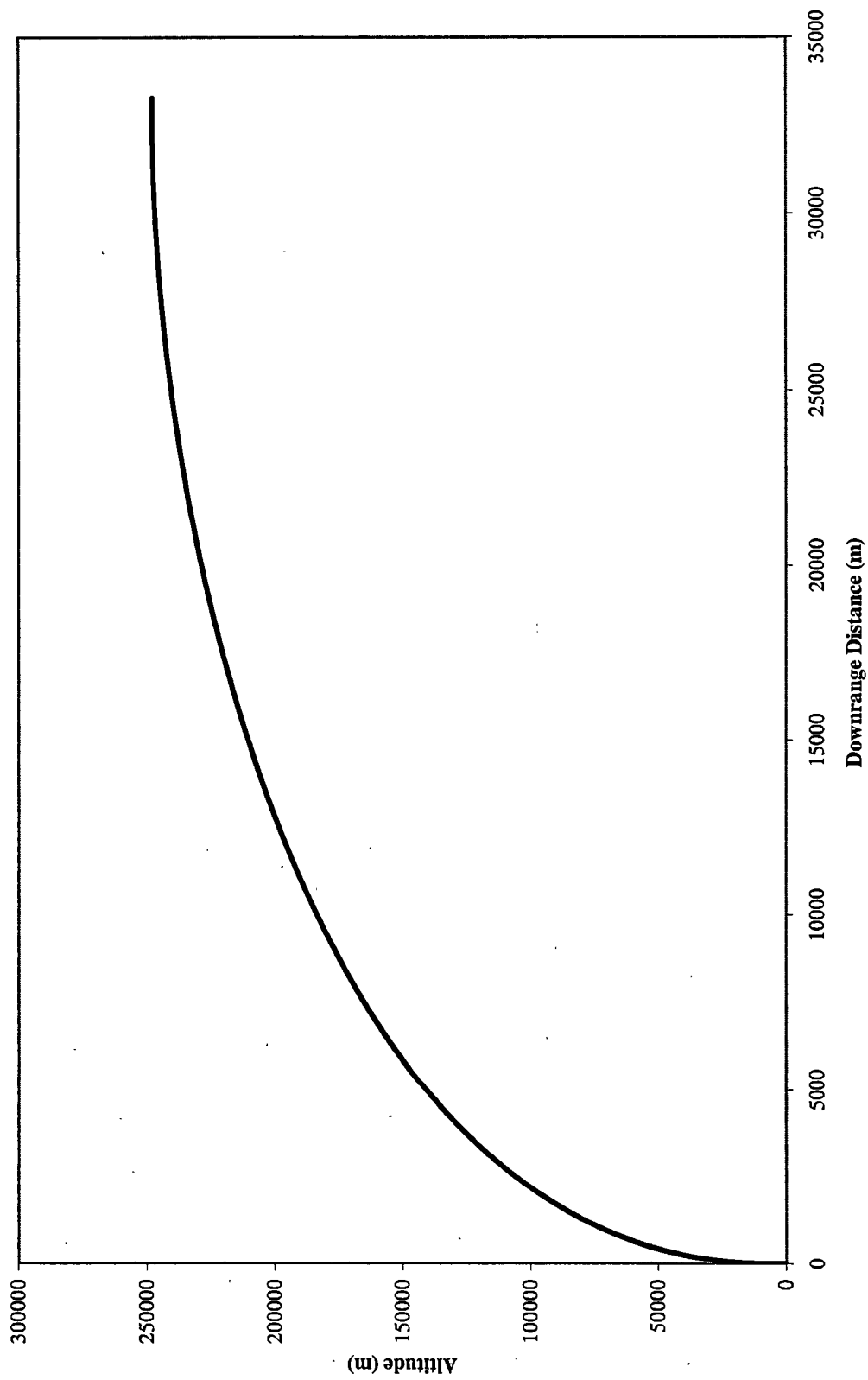
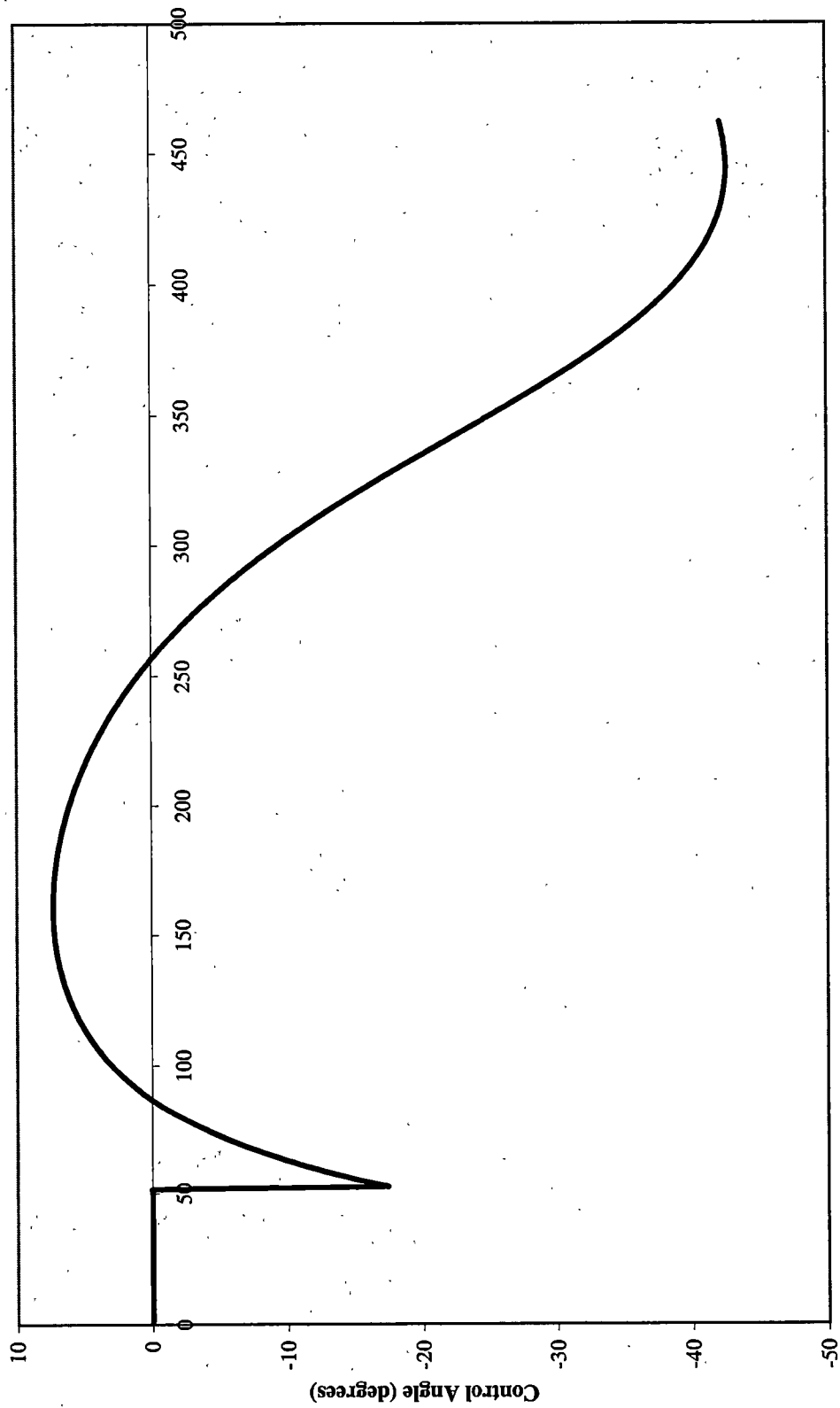


Figure 2.5.1: Trajectory for PAW Ascent



Time (s)

Figure 2.5.2: Control Angle History for PAW Ascent

of fuel remaining. This amount of fuel remaining corresponds to a ΔV of 796.93 m/s available for post ascent orbital maneuvering. This is less than the 1217.053 m/s required to match orbits with the ERV. As a result, the PAW ascent strategy must be ruled out as a viable method to accomplish the MAV mission.

2.5.2 Coast to Orbit Ascent

Both the second and third cases involve shutting the engine off at a point where drag effects from the Martian atmosphere can be neglected. The altitude selected in this study is 150 km, the altitude at which the atmospheric drag forces on the vehicle can be neglected [14]. The maneuvers that occur for orbit circularization and Hohmann style maneuvers require relatively small energy changes when compared to the magnitude of ΔV required in the ascent. For this purpose the orbital maneuvering that occurs post ascent is assumed to be impulsive. A coast phase following powered ascent is operationally attractive, as it gives the crew time to alter their trajectory if any deviation from the optimal trajectory had occurred during ascent.

The second case is based the spacecraft arriving at the cutoff altitude in a proper velocity and path angle to coast to an apoapsis of 250 km, at which point a specified value of ΔV is required to circularize the orbit. This involves launching the spacecraft to some point on the elliptical orbit that is co-tangential to the 250 km altitude circular orbit and the 150 km atmospheric limit. If the circularization maneuver is not performed at the 250 km apoapsis altitude of its coast orbit, the spacecraft must safely clear Mars and its atmosphere at the periapsis point of the cotangential orbit in order to return to the circularization altitude. The primary driver for the coast orbit periapsis altitude is the

magnitude of ΔV to be performed in the circularization maneuver. As can be seen in figure 2.5.3 a circularization maneuver ΔV of 25 m/s will allow the coast orbit periapsis to have an altitude of 149.17 km, just inside the 150 km atmospheric limit. This dictates that the engine cutoff altitude must be greater than 150 km. Utilizing the amount of fuel left post ascent as a criteria for a useful ascent strategy, our choice of engine cutoff altitude is limited. Figure 2.5.4 shows that a trajectory with a lower cutoff altitude consumes less fuel in the ascent, while trajectories with engine cutoff altitudes higher than 180 km do not leave the MAV with enough fuel to achieve the required ΔV of 1217.053 m/s to match orbits with the ERV. For this reason a trajectory with a cutoff altitude of 160 km and a circularization maneuver of 25 m/s was assumed in this study.

The procedure to calculate the flight conditions at burnout is based upon finding the radial and tangential components of velocity at an altitude of 160 km along the orbit that is cotangential with the 250 km circular orbit and the 150 km atmosphere limit. This is done by the following set of equations [13]. The first step in coast orbit determination is calculating the orbital energy constant h , and the Kepler area constant C , according to the equations:

$$h = v^2 - \frac{2GM}{r}$$

$$C = vr$$

where v is the difference between the circular orbit speed at the 250 km altitude and the ΔV for circularization and r is the radius at 250 km altitude. From this the eccentricity of the cotangential orbit can be calculated from the following equation:

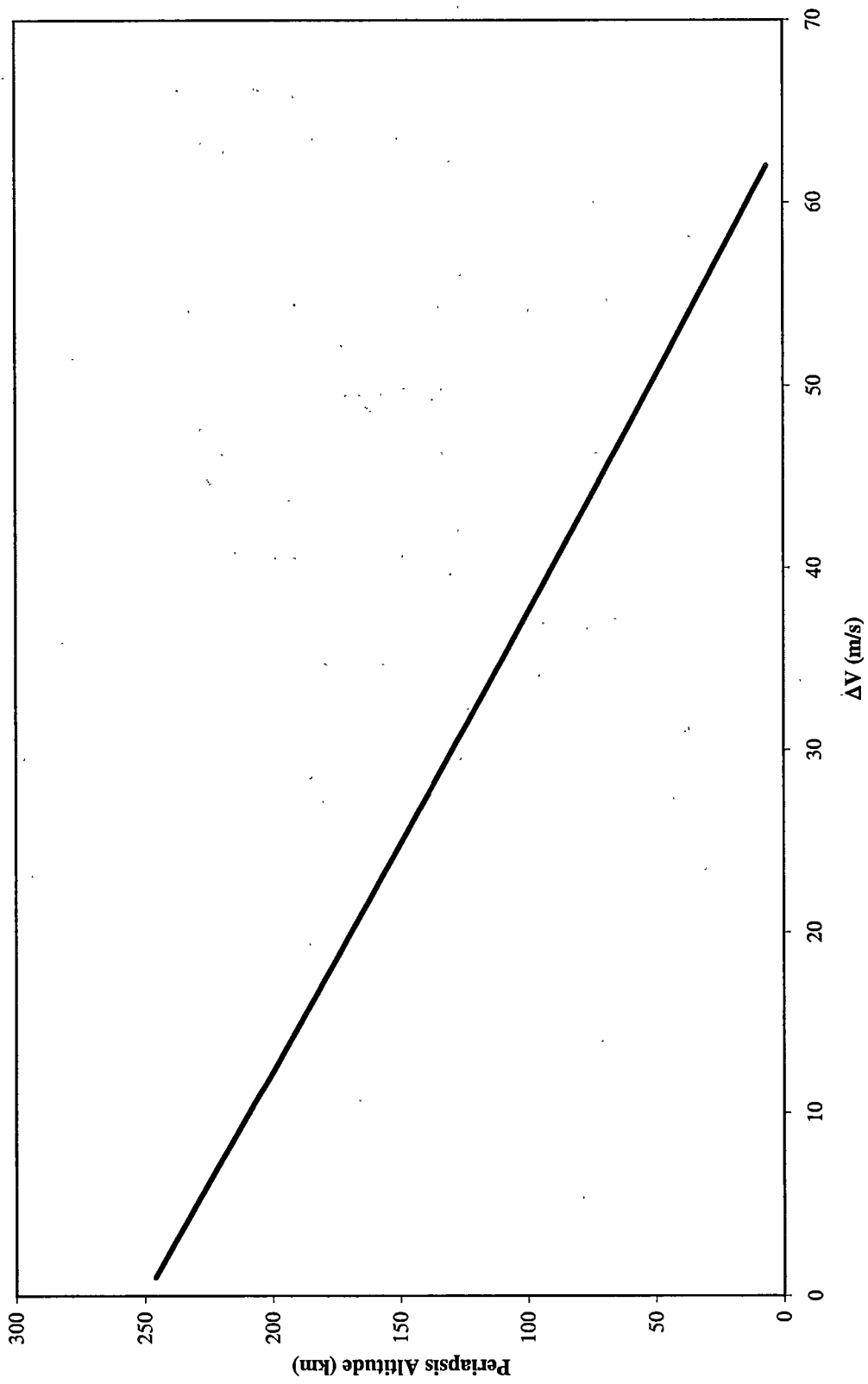


Figure 2.5.3: Periapsis Altitude of Coast Orbit vs. Circularization ΔV

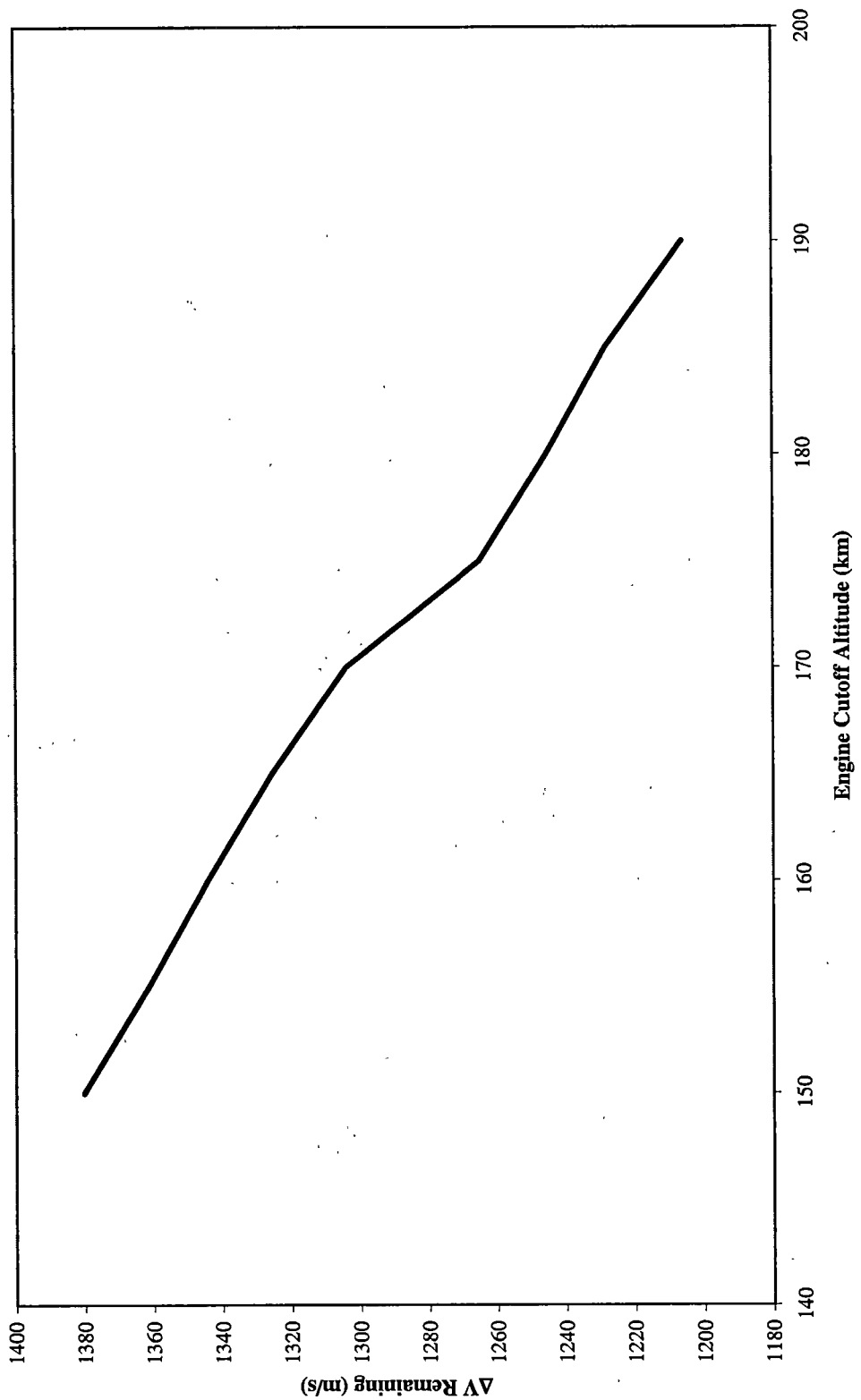


Figure 2.5.4: ΔV Remaining vs. Engine Cutoff Altitude for Coast to Orbit Ascent

$$e = \sqrt{1 + \frac{C^2 h}{GM^2}}$$

Having the eccentricity of the cotangential orbit yields the periapsis radius of the cotangential orbit through the following relation:

$$r_p = r_{250km} \frac{1-e}{1+e}$$

The semimajor axis of the cotangential orbit is then found by the equation:

$$a = \frac{r_p}{|e-1|}$$

The path velocity at the engine cutoff point is then calculated by the relation:

$$v_{cut} = \sqrt{\frac{GM}{r_{cut}}} \sqrt{2 - \frac{r_{cut}}{a}}$$

The tangential and radial components of velocity at the cutoff altitude are then found by the following equations:

$$v_{\theta} = \frac{r_{250km} (v_{circ250km} - \Delta v)}{r_{cut}}$$

$$v_r = \sqrt{v_{cut}^2 - v_{\theta}^2}$$

The trajectory followed by the spacecraft for the coast to orbit ascent is shown in figure 2.5.5. The highest acceleration felt on the MAV at engine shutdown has a value of 20.78 m/s, corresponding to 2.11 Earth gravities and 5.31 Mars gravities. The control angle history for coast to orbit ascent is shown in figure 2.5.6. The largest absolute value for control angle is 27.99 degrees. This is less than the largest control angle required for the PAW ascent, 42.65 degrees, but is still large enough to be accomplished only by maneuvering the entire vehicle at an angle to its flight path.

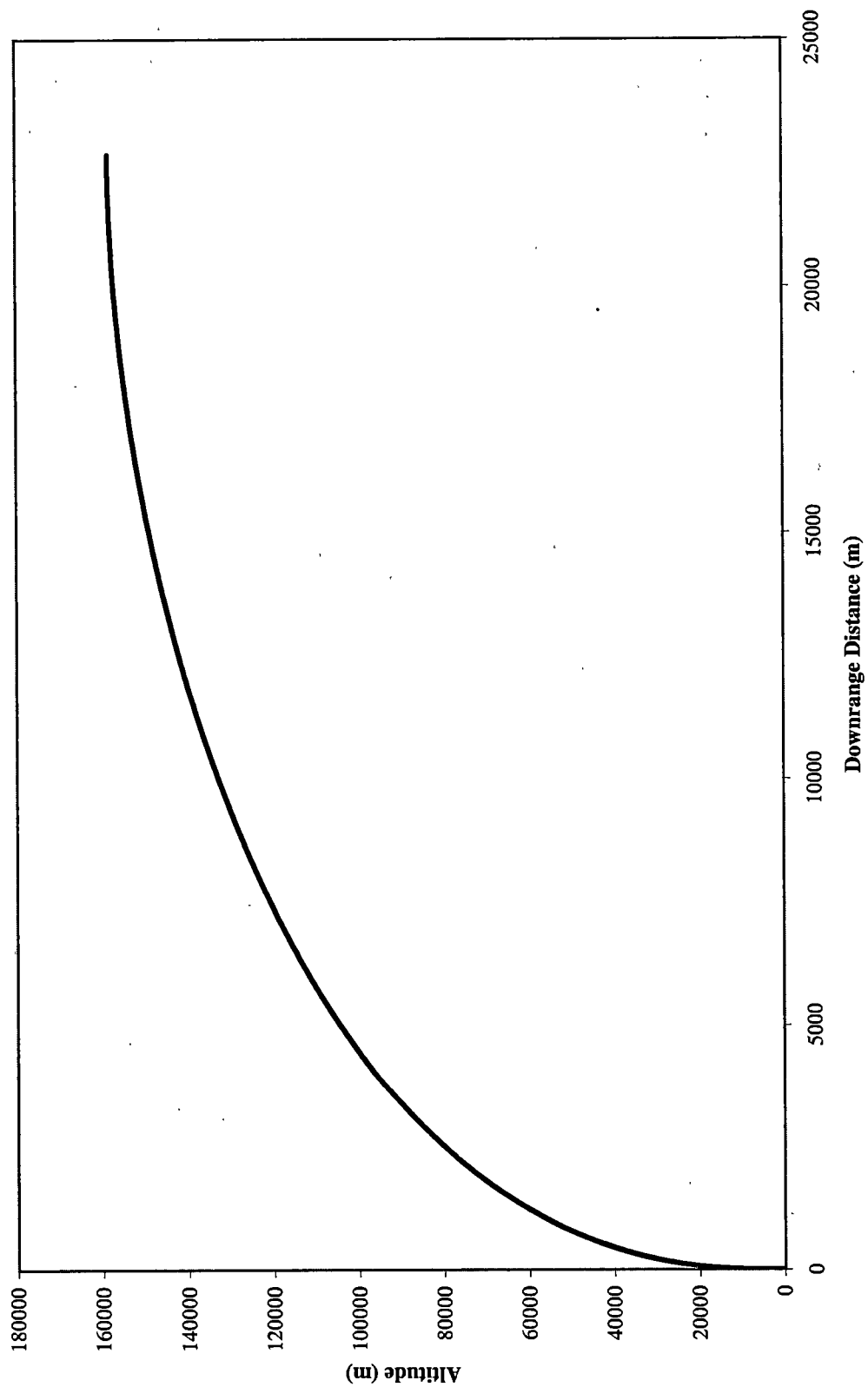


Figure 2.5.5: Trajectory for Coast to Orbit Ascent

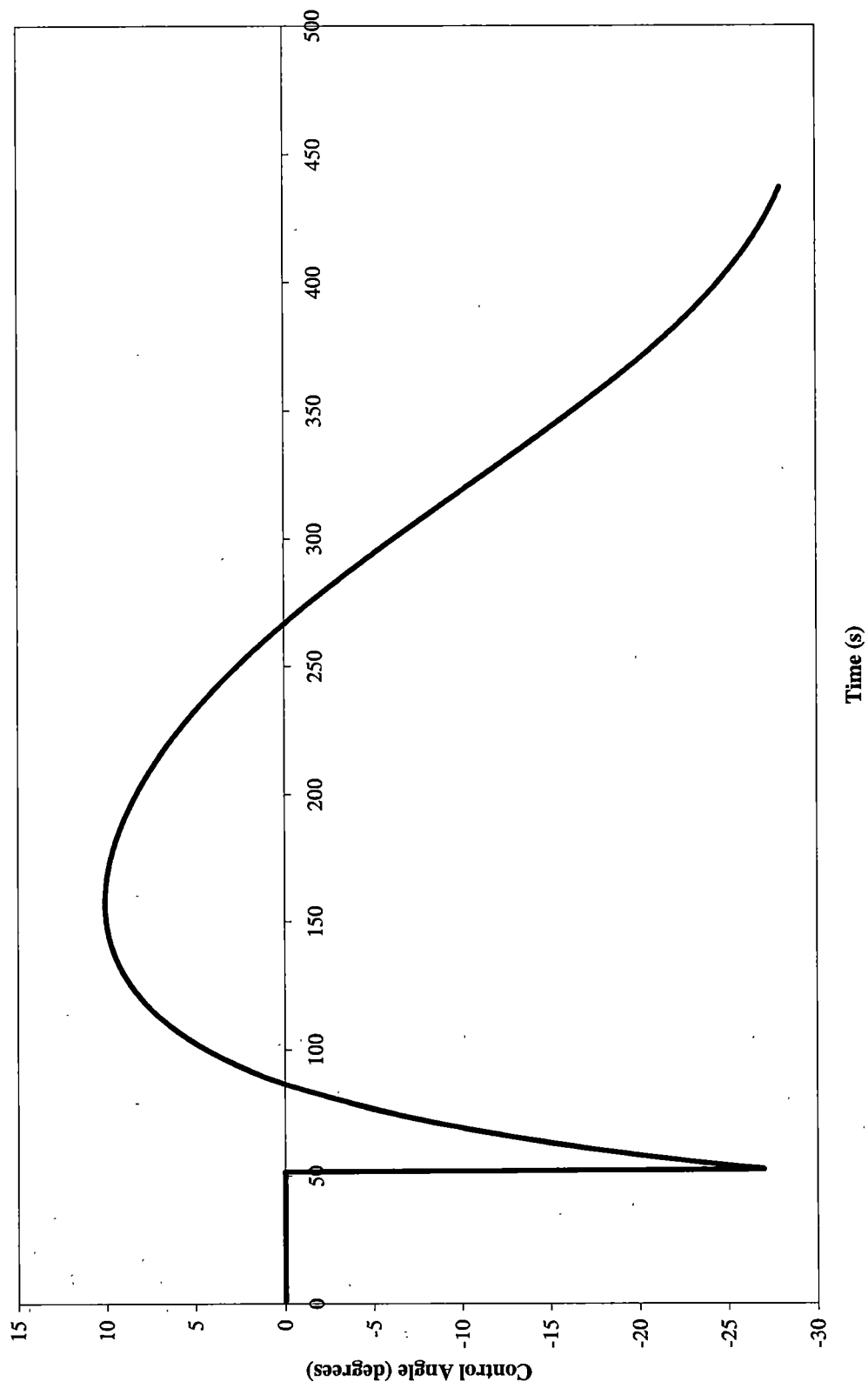


Figure 2.5.6: Control Angle History for Coast to Orbit Ascent

The coast to orbit strategy with an engine cutoff altitude of 160 km requires the engines to run for 437.089 seconds, leaving 4303.87 kg of propellant available after engine shutoff. The circularization maneuver of 25 m/s of ΔV consumes an additional 66.77 kg of propellant, leaving 4237.10 kg of propellant. This corresponds to an available ΔV of 1324.82 m/s. As this number is more than the ΔV required for matching orbits with the ERV, it can be concluded that coast to orbit is a viable launch strategy. An operational drawback to this strategy is that the launch must be carefully timed to place the MAV in the 250 km altitude circular orbit to arrive at the periapsis point of the ERV orbit.

2.5.3 Low Orbit with Hohmann Transfer Ascent

The third approach to ascending to orbit is an outgrowth of the coast to orbit strategy. It was observed from the coast to orbit strategy that a lower engine cutoff altitude reduces the amount of fuel consumed in the ascent. Rather than launch to an arbitrary point along the cotangential elliptical orbit, the third launch strategy places the MAV in a circular orbit at 150 km altitude. From this point a Hohmann transfer ellipse is used to raise the orbit to the desired 250 km altitude. Hohmann transfer is the optimum minimum energy method for raising the orbit of a spacecraft. This procedure is operationally the most attractive, as the crew can spend a given amount of time in low Mars orbit before executing the Hohmann transfer to the higher 250 km altitude orbit. This variable amount of time spent in low Mars orbit relaxes the need to launch at a specified time in order to arrive at the periapsis point of the ERV orbit, a problem that arises in the coast to orbit launch strategy.

The magnitude of ΔV needed to raise the circular orbit to the altitude of 250 km for rendezvous with the ERV are calculated by the equations for a Hohmann transfer [15].

$$\Delta V_1 = \sqrt{\frac{2GM}{r_{150\text{km}}} - \frac{2GM}{r_{150\text{km}} + r_{250\text{km}}}} - \sqrt{\frac{GM}{r_{150\text{km}}}}$$

$$\Delta V_2 = \sqrt{\frac{GM}{r_{250\text{km}}}} - \sqrt{\frac{2GM}{r_{250\text{km}}} - \frac{2GM}{r_{150\text{km}} + r_{250\text{km}}}}$$

The magnitudes of these two maneuvers are found to be 24.97 m/s and 24.79 m/s, respectively.

The trajectory followed by the spacecraft for the low orbit with Hohmann transfer ascent strategy is shown in figure 2.5.7. The ascent to low orbit with Hohmann transfer produces accelerations and control angles nearly identical to that of coast to orbit ascent. The highest acceleration felt on the MAV at engine shutdown has a value of 20.46 m/s, corresponding to 2.08 Earth gravities and 5.23 Mars gravities. The control angle history for this ascent strategy is shown in figure 2.5.8. The largest absolute value for control angle is 26.93 degrees.

The ascent to low orbit with Hohmann transfer strategy requires the engines to run for 434.328 seconds, leaving 4523.04 kg of fuel in the tanks at engine cutoff. The Hohmann maneuver to raise the orbit to 250 km expends an additional 133.36 kg of propellant, leaving 4389.68 kg of propellant remaining. This corresponds to 1364.74 m/s of ΔV available to match orbits with the ERV and perform the rendezvous. This may seem only a marginal improvement over the coast to orbit ascent strategy, saving 152.58 kg of propellant and allowing 39.92 m/s more ΔV . The result, however, shows that

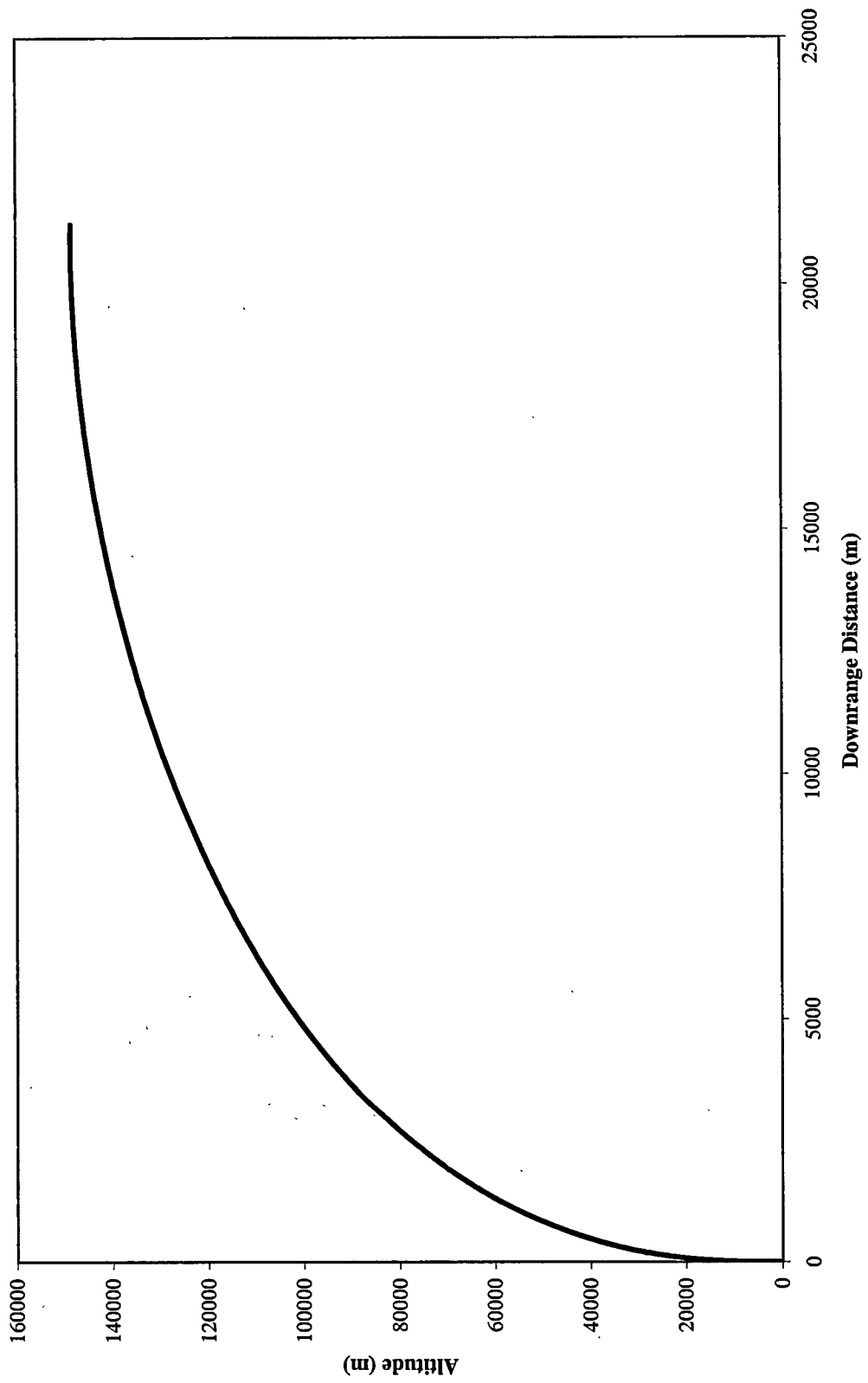
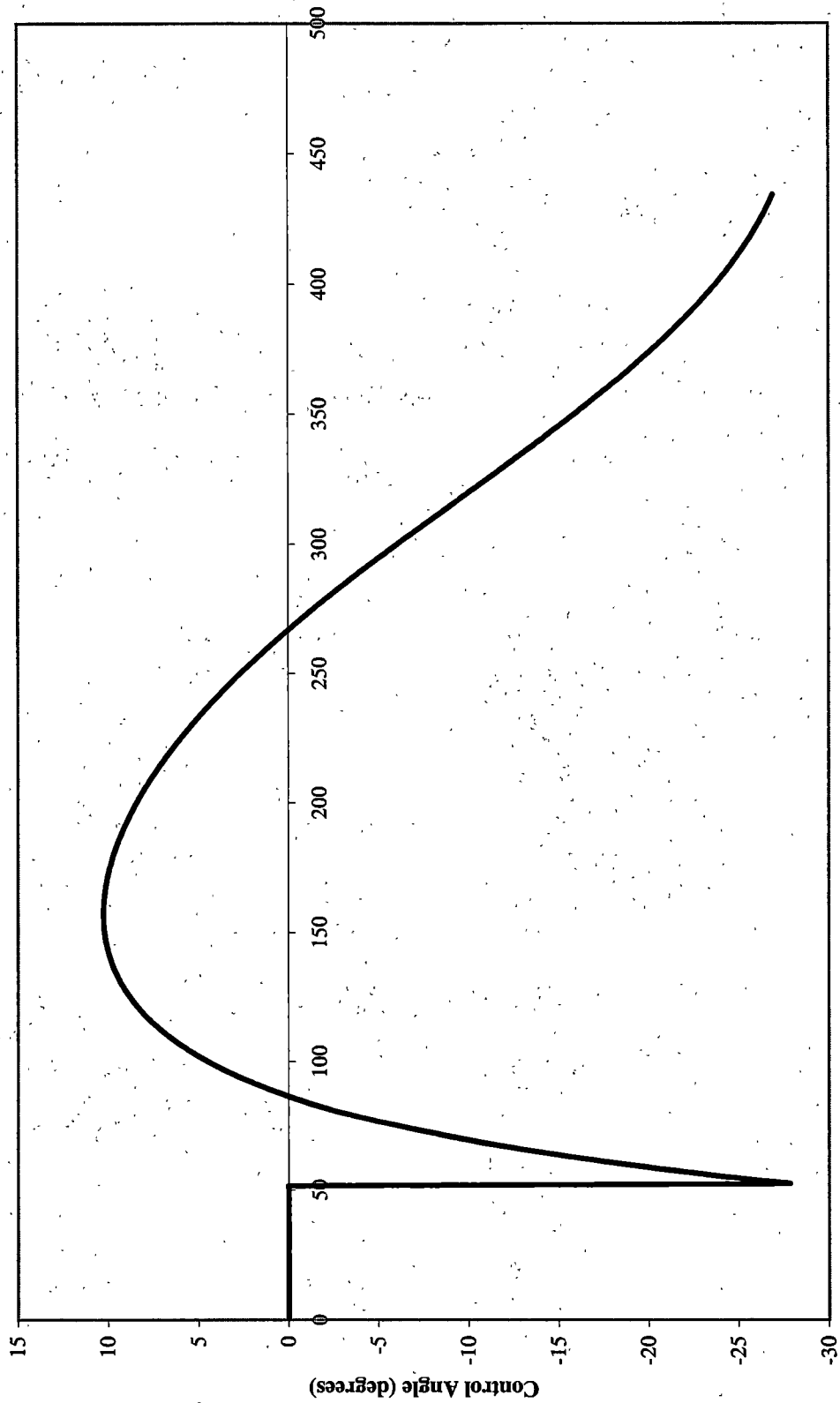


Figure 2.5.7: Trajectory for Ascent with Hohmann Maneuver



Time (s)

Figure 2.5.8: Control Angle History for Ascent with Hohmann Maneuver

ascent to a low circular orbit combined with the use of a Hohmann transfer to raise the orbit to its final desired altitude is the most efficient ascent strategy.

3. RENDEZVOUS ANALYSIS

3.1 Equations of Relative Motion

Once in orbit the MAV must rendezvous with the waiting ERV, into which the crew must transfer themselves and their scientific payload from the surface of Mars, prior to preparing for the voyage to Earth. Rendezvous between these the MAV and the ERV is accomplished through matching the orbits of the two vehicles. This is performed through two impulsive maneuvers, the first of which takes the MAV to the vicinity of the ERV and the second of which nulls the relative velocity between the two vehicles. Determining the ΔV needed to perform these maneuvers is achieved by a study of the relative motions of the two vehicles.

The first step in the analysis is to determine the relative position of the two spacecraft. A moving coordinate frame is attached to the ERV, while the coordinate frame originating at the center of Mars is assumed to be inertial. Figure 3.1.1 shows a diagram of the coordinate system used in the derivation of the equations of relative motion between the two spacecraft.

The relative position ρ is represented by the equation

$$\mathbf{r} = \mathbf{r}_T + \rho$$

where \mathbf{r} and \mathbf{r}_T are the positions of the MAV and ERV in relation to the center of Mars.

This equation is differentiated with respect to the inertial coordinate system, yielding

[16]:

$$\ddot{\mathbf{r}} = \ddot{\mathbf{r}}_T + \ddot{\rho} + 2 \cdot (\omega \times \dot{\rho}) + \dot{\omega} \times \rho + \omega \times \omega \times \rho$$

where $\ddot{\mathbf{r}}$ is the inertial acceleration of the MAV, $\ddot{\mathbf{r}}_T$ the inertial acceleration of the ERV, $\ddot{\rho}$

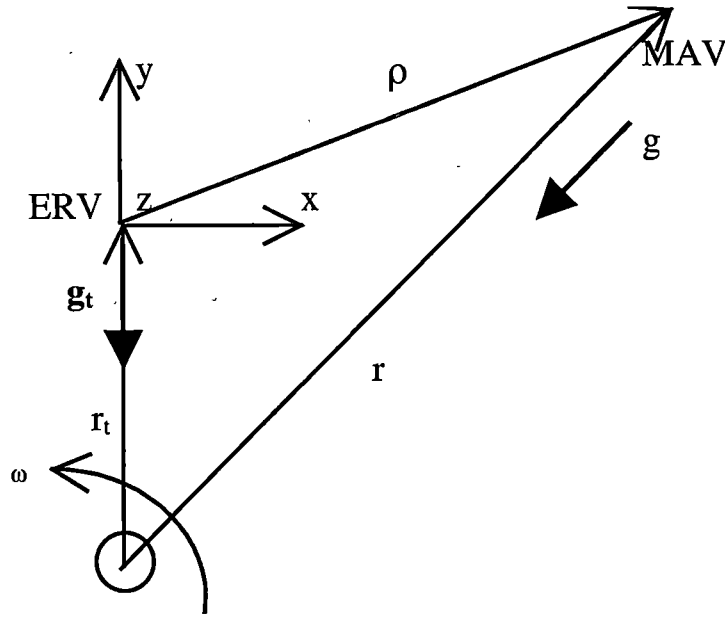


Figure 3.1.1 Coordinate System for Rendezvous

the acceleration of the MAV relative to the ERV, $2 \cdot (\omega \times \dot{\rho})$ the Coriolis acceleration, $\dot{\omega} \times \rho$ the Euler acceleration and $\omega \times (\omega \times \rho)$ the centripetal acceleration.

By neglecting the small gravitational acceleration between the two vehicles their inertial acceleration can be viewed as the sum of the gravitational acceleration caused by Mars and the applied accelerations caused by powered maneuvers. Inserting these into the inertial acceleration equation, resolving it into x, y, and z coordinates, and solving it for the relative acceleration yields:

$$\begin{aligned} \ddot{\rho}_x &= g_x - g_{Tx} + \frac{F_x}{m} + 2\omega\dot{\rho}_y + \dot{\omega}\rho_y + \omega^2\rho_x \\ \ddot{\rho}_y &= g_y - g_{Ty} + \frac{F_y}{m} - 2\omega\dot{\rho}_x - \dot{\omega}\rho_x + \omega^2\rho_y \\ \ddot{\rho}_z &= g_z - g_{Tz} + \frac{F_z}{m} \end{aligned}$$

It is assumed that the radial positions of the MAV and the beginning of the rendezvous are not significantly different. This allows for the gravitational term in the above equations to be approximated as [16]:

$$\begin{aligned} g_x &= -g \left(\frac{\rho_x}{r} \right) \approx -g_T \left(\frac{\rho_x}{r_T} \right) \\ g_y &= -g \left(\frac{\rho_y + r_T}{r} \right) \approx -g_T \left(1 - \frac{2\rho_y}{r_T} \right) \\ g_z &= -g \left(\frac{\rho_z}{r} \right) \approx -g_T \left(\frac{\rho_z}{r_T} \right) \end{aligned}$$

Inserting these relations into the relative acceleration equations and noting that the ERV is accelerating only in a negative y direction towards Mars yields the following expressions:

$$\begin{aligned} \ddot{\rho}_x &= -g_T \left(\frac{\rho_x}{r_T} \right) + \frac{F_x}{m} + 2\omega\dot{\rho}_y + \dot{\omega}\rho_y + \omega^2\rho_x \\ \ddot{\rho}_y &= 2g_T \left(\frac{\rho_y}{r_T} \right) + \frac{F_y}{m} - 2\omega\dot{\rho}_x - \dot{\omega}\rho_x + \omega^2\rho_y \\ \ddot{\rho}_z &= -g_T \left(\frac{\rho_z}{r_T} \right) + \frac{F_z}{m} \end{aligned}$$

It is observed that for the case of circular orbits the value of $\dot{\omega}$ is equal to zero and g_T/r_T can be expressed as ω^2 . Taking these relations into account the relative acceleration equations could be simplified into the following form:

$$\begin{aligned} \ddot{\rho}_x &= \frac{F_x}{m} + 2\omega\dot{\rho}_y \\ \ddot{\rho}_y &= \frac{F_y}{m} - 2\omega\dot{\rho}_x + 3\omega^2\rho_y \\ \ddot{\rho}_z &= \frac{F_z}{m} - \omega^2\rho_z \end{aligned}$$

A simple solution can be sought to these equations through a harmonic oscillator approach [15]. The equations in their above form have been widely used for rendezvous applications in Earth orbit, as most rendezvous occur in circular or nearly circular orbits [17]. For the case of the target satellite in an elliptical orbit, such as the ERV in its parking orbit around Mars, the equations prove to be more complex.

The gravitational acceleration of the ERV can be expressed as the gravitational parameter over the square of the radius, GM/r_T^2 . The angular velocity and acceleration of the ERV coordinate system are equal to the first and second derivatives with respect to time of the true anomaly v of the ERV. It can also be shown that the instantaneous radius of the ERV, r_T , is a function of the true anomaly and the orbital parameters of eccentricity and perigee radius by the following relation [13]:

$$r_T = \frac{r_p(1+e)}{1+e \cdot \cos(v)}$$

We can now write the spatial acceleration equations along with an expression for the second derivative with respect to time for the true anomaly in the following form:

$$\begin{aligned} \ddot{\rho}_x &= \frac{-GM \cdot \rho_x}{\left(\frac{r_p(1+e)}{1+e \cdot \cos(v)}\right)^3} + \frac{T_x}{m} + 2\dot{v}\dot{\rho}_y + \ddot{v}\rho_y + (\dot{v})^2\rho_x \\ \ddot{\rho}_y &= \frac{2 \cdot GM \cdot \rho_y}{\left(\frac{r_p(1+e)}{1+e \cdot \cos(v)}\right)^3} + \frac{T_y}{m} - 2\dot{v}\dot{\rho}_x - \ddot{v}\rho_x + (\dot{v})^2\rho_y \\ \ddot{\rho}_z &= \frac{-GM \cdot \rho_z}{\left(\frac{r_p(1+e)}{1+e \cdot \cos(v)}\right)^3} + \frac{T_z}{m} \end{aligned}$$

$$\ddot{v} = \frac{-2 \cdot GM \cdot e \cdot \sin(v)}{\left(\frac{r_p(1+e)}{1+e \cdot \cos(v)} \right)^3}$$

3.2 Solution Method

The equations for relative acceleration are second order derivatives, but they can be solved by Runge-Kutta integration by treating them as a set of six first order differential equations. Taken along with the two differential equations for true anomaly of the ERV, this results in the following set of expressions:

$$\frac{d\rho_x}{dt} = \dot{\rho}_x$$

$$\frac{d\dot{\rho}_x}{dt} = \frac{-GM \cdot \rho_x}{\left(\frac{r_p(1+e)}{1+e \cdot \cos(v)} \right)^3} + \frac{T_x}{m} + 2\dot{v}\dot{\rho}_y + \ddot{v}\rho_y + (\dot{v})^2\rho_x$$

$$\frac{d\rho_y}{dt} = \dot{\rho}_y$$

$$\frac{d\dot{\rho}_y}{dt} = \frac{2 \cdot GM \cdot \rho_y}{\left(\frac{r_p(1+e)}{1+e \cdot \cos(v)} \right)^3} + \frac{T_y}{m} - 2\dot{v}\dot{\rho}_x - \ddot{v}\rho_x + (\dot{v})^2\rho_y$$

$$\frac{d\rho_z}{dt} = \dot{\rho}_z$$

$$\frac{d\dot{\rho}_z}{dt} = \frac{-GM \cdot \rho_z}{\left(\frac{r_p(1+e)}{1+e \cdot \cos(v)} \right)^3} + \frac{T_z}{m}$$

$$\frac{dv}{dt} = \dot{v}$$

$$\frac{d\dot{v}}{dt} = \frac{-2 \cdot GM \cdot e \cdot \sin(v)}{\left(\frac{r_p(1+e)}{1+e \cdot \cos(v)} \right)^3}$$

There are a total of eight equations, the first six of which govern the spacecraft relative positions and velocities in three dimensions. These six equations are dependent in turn upon the two equations for the velocity and acceleration of the true anomaly of the ERV. The initial relative position is known along with the velocity and acceleration of the true anomaly. Table 3.2.1 contains a list of the boundary value conditions for the rendezvous problem. The required initial relative velocity in three dimensions is unknown. The solution to this boundary value problem requires three known final conditions, which exist in the form of the desired final relative position between the two vehicles. These final distances between the spacecraft have a value of zero in order to allow a rendezvous and docking to occur.

For this study it is assumed that the MAV maneuvers are impulsive, that is they occur instantaneously. Impulsive maneuvers allow the acceleration terms in the differential equations to be disregarded in the Runge-Kutta integration. Rendezvous maneuvers between spacecraft within several kilometers of each other are typically

Table 3.2.1: Boundary Value Conditions for Rendezvous Problem

Variable	Initial Condition	Final Condition
Relative position x	known	known
Relative position y	known	known
Relative position z	known	known
Relative velocity x	unknown	unknown
Relative velocity y	unknown	unknown
Relative velocity z	unknown	unknown

measured in the tens of meters per second of ΔV , so assuming that the rendezvous maneuvers are impulsive is a close approximation of actual spacecraft operation [15].

The ΔV required by the MAV is found by subtracting the MAV inertial velocity from the sum of the ERV inertial velocity and the relative velocity, given by the equation:

$$\Delta V = V_{rel} - (V_{ERV} - V_{MAV} + \omega \times r)$$

The second maneuver, needed to null the relative velocities between the two spacecraft once they are at zero distance, can be found easily by examining the relative velocity value contained in the final iteration of the Runge-Kutta integration. In this way the required ΔV for each rendezvous maneuver can be specified. The boundary value problem is solved over a range of times in which it is desired for a rendezvous to occur.

In actual operation the relative range and velocity between the two spacecraft would be measured by rendezvous radar. For the purposes of the program included in this study the range and velocity data is calculated from the orbital characteristics of the two spacecraft.

3.3 Rendezvous Calculation Results

Having ascended into orbit on a trajectory timed to place them in the vicinity of the ERV as it passes through the periapsis of its highly eccentric orbit, the MAV must complete the terminal rendezvous. There are two primary methods to achieve this goal.

The first rendezvous strategy, the non co-orbital rendezvous, involves just two impulsive maneuvers. The MAV, in its circular orbit with ERV nearby at its periapsis point, calculates and performs a combined maneuver that both matches the MAV orbit to

that of the ERV and begins the terminal rendezvous. A small second maneuver is then performed to complete the rendezvous.

The second rendezvous strategy, the co-orbital rendezvous, involves three separate impulsive maneuvers. The MAV performs a Hohmann-style tangential maneuver to alter its circular orbit to the eccentric orbit the ERV is in. The two spacecraft are now in relatively close range (100 km or less apart) on similar orbits. The two maneuvers needed to complete the terminal rendezvous are then calculated and performed.

Although the method of analysis is able to handle relative distances in all three directions, for this study it was assumed that the MAV has been launched into a coplanar orbit with the ERV. This eliminates any z direction displacements between the two vehicles. Obtaining the proper orbital inclination is best achieved at the launch, eliminating the need for a costly inclination change maneuver [15].

The corresponding ΔV for this rendezvous in a desired time is calculated for each minute in a two hour span. The optimal desired time for a rendezvous to occur in is chosen based upon which time provides the minimal ΔV .

It should be understood that the rendezvous study taken here is made to simply quantify the magnitude of performance needed by the MAV to achieve a rendezvous. The actual circumstances of rendezvous, the positions and velocities of the spacecraft at a particular time, are subject to change from planned values because of a variety of influences. As mentioned before, the ascent would need careful planning to place the MAV as near as possible to the ERV to facilitate a successful rendezvous.

3.3.1 Non Co-orbital Rendezvous Case

The first case run for non co-orbital rendezvous involves the MAV in its 250 km altitude circular orbit at the periapsis point of the ERV orbit. The ERV itself is 1 degree of true anomaly ahead of the MAV. The program written to solve the problem calculates the relative distances between the two spacecraft measured in the ERV body centered coordinate system based on these orbital parameters. The distances between the two spacecraft are an x direction displacement of 62.135 km, a y direction displacement of -0.787 km, and a z direction displacement of 0.0 km, corresponding to a total distance between the two spacecraft of 62.136 km. Figure 3.3.1 shows the ΔV for each maneuver and the total ΔV required for rendezvous versus the desired time for rendezvous to occur. The total ΔV for both the first and second rendezvous maneuvers is large for the first few minutes of desired time to rendezvous starting at approximately 3.25 km/s. As the desired time to rendezvous increases, however, the total ΔV for the maneuver asymptotically approaches a value of 1.263 km/s.

The second case run for non co-orbital rendezvous involves the MAV in the same position as before, but the ERV is now 1 degree of true anomaly behind the ERV. This translates to an x direction displacement of -62.135 km, a y direction displacement of -0.787 km, and a z direction displacement of 0.0 km, corresponding to a total distance between the two spacecraft of 62.136 km. Figure 3.3.2 shows the ΔV for each maneuver and the total ΔV required for rendezvous versus the desired time for rendezvous to occur. The total ΔV for the rendezvous is at 1.222 km/s for the first few minutes of desired time

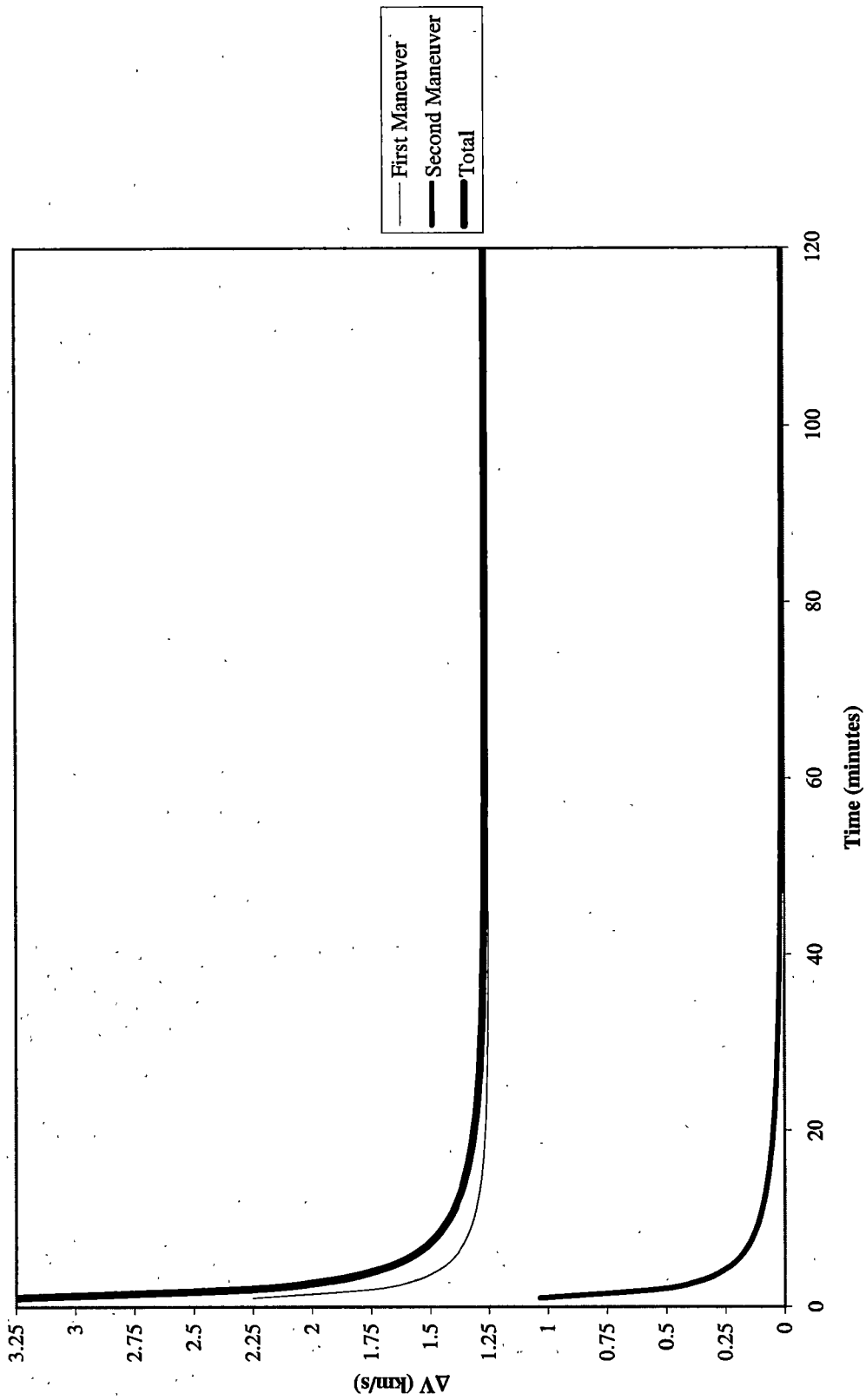


Figure 3.3.1: ΔV vs. Time for Non Co-orbital Rendezvous with ERV 62.13 km ahead of MAV

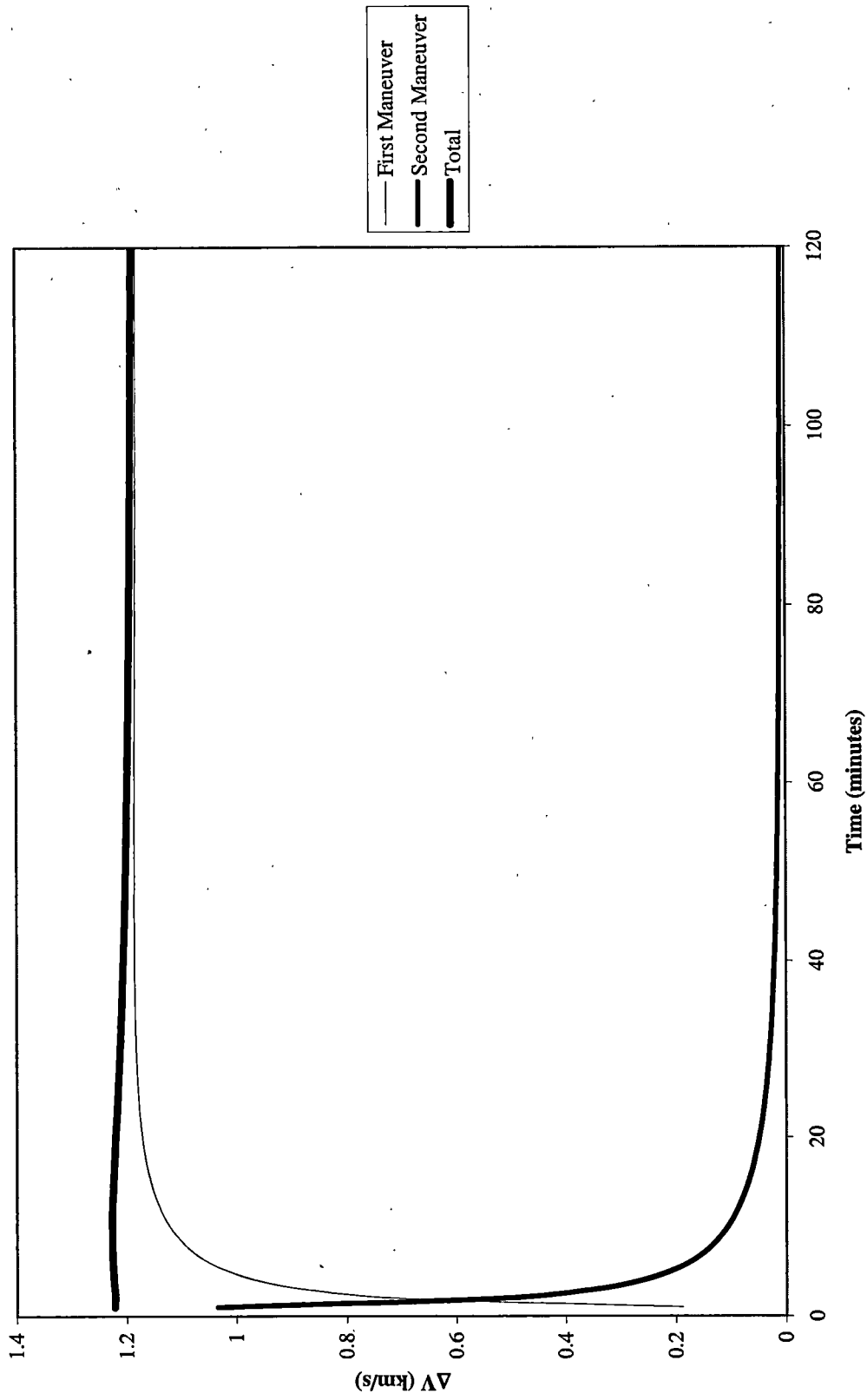


Figure 3.3.2: ΔV vs. Time for Non Co-orbital Rendezvous with ERV 62.13 km behind MAV

to rendezvous. As the desired time to rendezvous increases, the ΔV gradually falls to a value of 1.188 km/s.

3.3.2 Co-orbital Rendezvous Case

The case of co-orbital rendezvous assumes that the MAV has already performed the 1.217 km/s maneuver to match orbits with the ERV. The first case studied has the MAV at the periapsis point of the ERV orbit. The ERV is in the same position as in the first non co-orbital case, 1 degree of true anomaly ahead of the MAV. The distances between the two spacecraft are also the same as the first case of non-co-orbital rendezvous. The relative velocities between the spacecraft are different from the non co-orbital cases. Figure 3.3.3 shows the ΔV for each maneuver and the total ΔV required for rendezvous versus the desired time for rendezvous to occur. The total ΔV for the rendezvous reaches a minimum value of 0.049 km/s for the range of desired times for rendezvous between 60 and 70 minutes.

The second case of co-orbital rendezvous examined in this study has the MAV at the periapsis point with the ERV 1 degree of true anomaly behind the MAV. The distances between the spacecraft are the same as the second case of non co-orbital rendezvous. Figure 3.3.4 shows the ΔV for each maneuver and the total ΔV required for rendezvous versus the desired time for rendezvous to occur. The total ΔV is relatively large for small desired times to rendezvous, initially measured in the hundreds of meters per second. As the desired time to rendezvous increases the total ΔV for the rendezvous reaches a minimum value of 0.048 km/s for the range of times between 53 and 85 minutes.

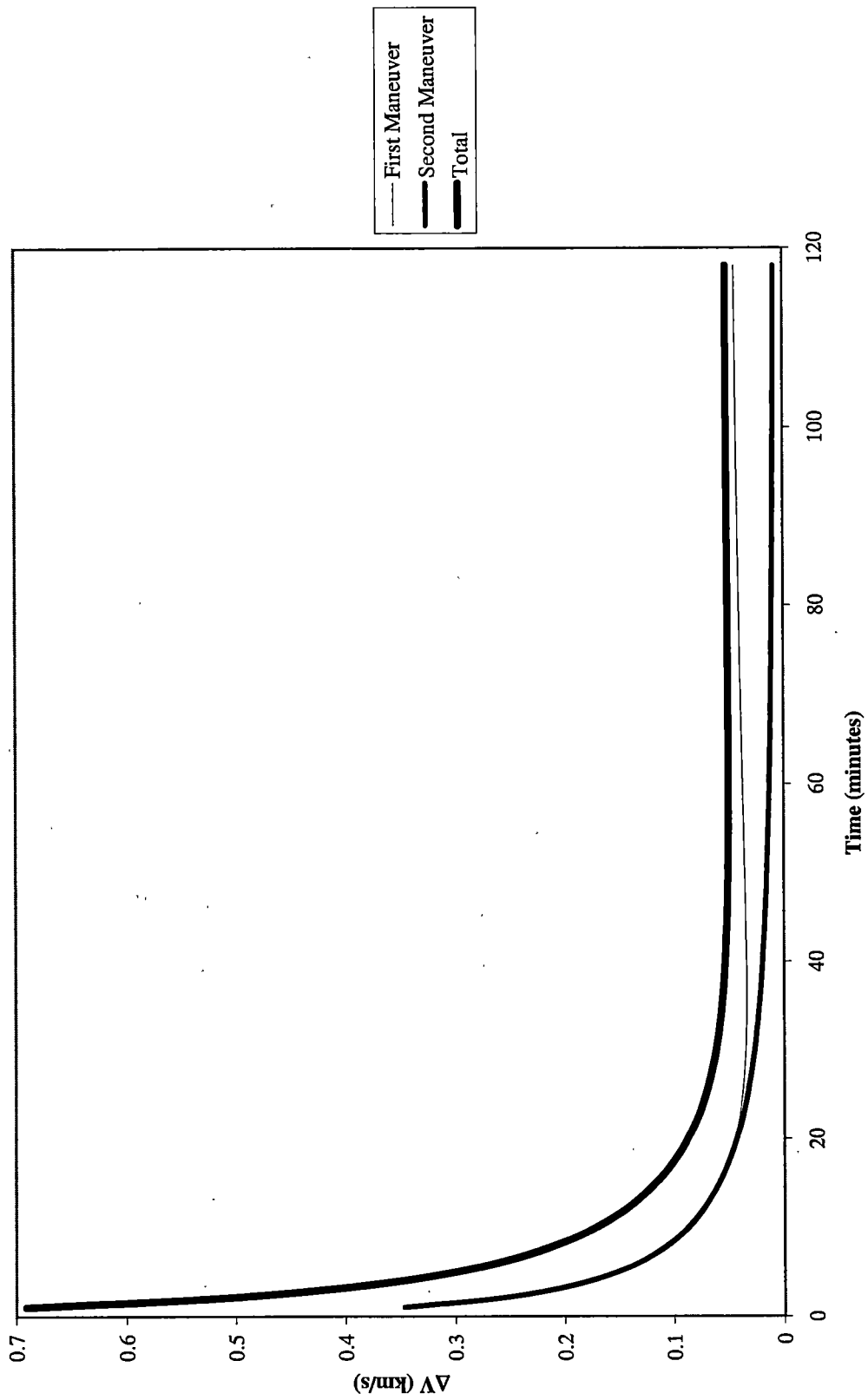


Figure 3.3.3: ΔV vs. Time for Co-orbital Rendezvous with ERV 62.13 km ahead of MAV

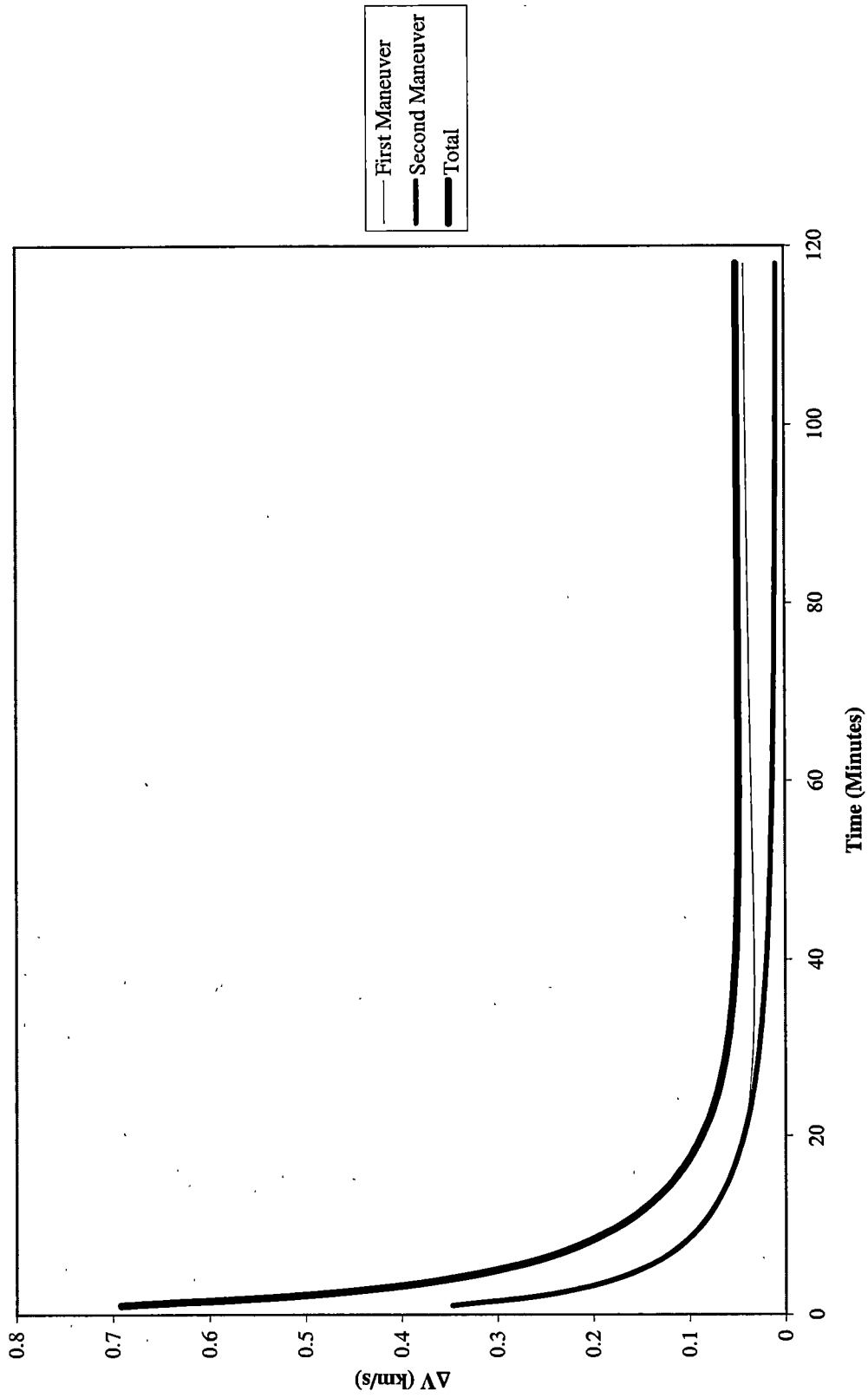


Figure 3.3.4: ΔV vs. Time for Co-orbital Rendezvous with ERV 62.13 km behind MAV

4. CONCLUSIONS

In this study, an initial estimate of required performance was sought for a MAV within the context of NASA's Mars DRM. Each phase of the MAV mission, ascent and rendezvous has been modeled, taking into account as many operational considerations as possible. For the first phase of the MAV mission, ascent from the Martian surface to orbit, three distinct ascent strategies were studied. The primary criteria used in judging the viability of each ascent strategy was the availability of post ascent propellant to match the MAV orbit with that of the ERV, a maneuver costing 1217.053 m/s. Table 4.1 shows the propellant remaining and the ΔV available at the end of the powered ascent for each strategy. The PAW ascent strategy leaves the MAV with insufficient propellant to match orbits with the ERV.

While both of the other launch strategies included in this study leave the MAV with sufficient propellant to match orbits with the ERV, table 4.1 shows that the low orbit with Hohmann transfer is the most efficient launch strategy.

The launching of the MAV on a low orbit with Hohmann transfer ascent strategy has several secondary benefits. The period of time that can be spent in the low orbit

Table 4.1: Summary of Launch Strategy Performance

Ascent Strategy	Propellant remaining (kg)	ΔV remaining (m/s)
PAW	2366.16	796.93
Coast to 160 km	4303.87	1324.82
Low Orbit with Hohmann	4389.68	1364.74

before transfer to the 250 km circular orbit prior to rendezvous allows for the relaxation of launch windows. Another benefit to the low orbit with Hohmann transfer is that it can be accomplished with the lowest acceleration on the spacecraft. For each ascent strategy it was found that the spacecraft would have to be flown at relatively large angles to its velocity vector. The side loading produced by flying the MAV at an angle to its flight path would add structural weight to the vehicle. It was found in the study that the low orbit with Hohmann transfer produced the smallest control angles of the three ascent strategies in the study. Table 4.2 shows the comparison of acceleration and control angle among the three ascent strategies.

For the second phase of the MAV mission, the requirements for terminal rendezvous to occur quantified through a study of the equations of relative motion between the two spacecraft. Typical rendezvous conditions, occurring at the periapsis of the ERV orbit, were modeled. Four different cases were studied; two with the ERV and the MAV in their dissimilar orbits, and two cases occurring after the MAV had matched orbits with the ERV. Table 4.3 gives a comparison of the minimum required ΔV and its corresponding desired time to rendezvous for each of the four cases.

Table 4.2: Summary of Acceleration and Control angle Characteristics

Ascent Strategy	Maximum g (Earth)	Maximum α (deg.)
PAW	2.46	42.65
Coast to 160 km	2.11	27.99
Low Orbit with Hohmann Transfer	2.08	26.93

Table 4.3: Summary of Rendezvous Performance

Rendezvous Case	Minimum ΔV (km/s)	Time (min.)
Non Co-orbital, ERV behind MAV	1.188	120
Non Co-orbital, ERV ahead of MAV	1.263	85
Co-orbital, ERV behind MAV	1.265	64
Co-orbital, ERV ahead of MAV	1.266	64

Note: For the co-orbital rendezvous cases, the 1.217 km/s ΔV required for orbit matching has been added to the terminal rendezvous ΔV .

For each rendezvous case it can be noted that the minimum ΔV is less than the 1.364 km/s ΔV available at the end of the low ascent with Hohmann transfer ascent strategy. As an initial performance estimate, this study has shown that the MAV, as it is described in the DRM documentation, is capable of performing the ascent and rendezvous with the ERV. Use of the low orbit with Hohmann transfer ascent strategy has been shown to be the most efficient method of achieving the MAV mission, as well as being the more operationally attractive and technically feasible method.

5. RECCOMENDATIONS FOR FURTHER STUDY

The results of this study could be made more realistic by the inclusion of aerodynamic effects on the vehicle as it passes through the Martian atmosphere on its journey to orbit. This would necessitate the inclusion of a Martian atmosphere model within the calculations. The Martian atmosphere, however, is not well defined at present, and further study is required before atmospheric effects could be included in this performance study. Due to the low density of the Martian atmosphere, its effect would be minimal on the ascending MAV. This allows the results of this study to be viewed as an accurate estimate of the required performance to complete the MAV mission.

An additional issue is the affect of acceleration on the crew following their six month exposure to zero gravity on the outbound trip to Mars and the 500 day exposure to Mars' limited gravity. Further study is required in the field of aerospace medicine concerning the effect of long-term exposure to micro- and low gravity on human performance. The need to limit acceleration experienced by the crew would lead to changes in the basic problem formulation. A throttleable thrust system would have to be mathematically modeled and constrained to work within set parameters. The optimization problem would change from the minimization of time to the minimization of propellant expended, with throttle as an additional control. Such a problem formulation is within the capabilities of the PMP.

LIST OF REFERENCES

LIST OF REFERENCES

1. Kos, L. D., "Human Mars Mission: Transportation Assessment", AIAA 98-5118, Defense and Civil Space Programs Conference & Exhibit, Huntsville, AL, 28 – 30 July 1998.
2. Drake, B. G. (editor), "Reference Mission 3.0 Addendum to the Human Exploration of Mars: The Reference Mission of the NASA Mars Exploration Study Team", Exploration Office Document EX13-98-036.
3. Zubrin, R. M. The Case for Mars, Simon & Schuster Inc., New York, NY, 1996
4. Hoffman, S.J. and Kaplan, D. I. (editors), "Human Exploration of Mars: The Reference Mission of the NASA Mars Exploration Study Team", NASA Special Publication 6107, July 1997.
5. Ehricke, K. A., Spaceflight, Volume II: Dynamics, D. Van Nostrand Company, Inc., Princeton, NJ, 1962.
6. Jezewski, D. J., "An Optimal, Analytic Solution to the Linear Gravity, Constant-Thrust Trajectory Problem", *AIAA Journal of Spacecraft and Rockets*, Vol. 8, No. 1, July, 1971, pp. 793-796.

7. McIntyre, J. E., "Guidance, Flight Mechanics, and Trajectory Optimization", NASA CR-1012, March, 1968.
8. Schindler, G. M., "Minimum Flight Time Paths", *Journal of the American Rocket Society*, Vol. 30, No. 4, April, 1960, pp. 352-355.
9. Sinha, S., "A Study to Evaluate STS Heads-Up Performance Employing a Minimum-Hamiltonian Optimization Strategy", NASA TP-2793, February, 1988.
10. Hocking, L. M., Optimal Control: An Introduction to the Theory with Applications, Oxford University Press, New York, NY, 1991.
11. Lewallen, J. M., Scwusch, O. A., and Tapley, B.D., "Coordinate System Influence on the Regularized Trajectory Optimization Problem", *AIAA Journal of Spacecraft and Rockets*, Vol. 8, No. 1, January, 1971, pp. 15-20.
12. Marec, J. P., Optimal Space Trajectories, Elsevier Scientific Publishing Company, Amsterdam, The Netherlands, 1979.
13. Ehricke, K. A., Spaceflight, Volume I: Environment and Celestial Mechanics, D. Van Nostrand Company, Inc., Princeton, NJ, 1962.

14. Johnston, M. D., Esposito, et al, "Mars Global Surveyor Aerobraking at Mars", AAS 98-112, 1998.
15. Wiesel, W. E., Spaceflight Dynamics, McGraw-Hill Inc., New York, NY, 1989.
16. Chobotov, V. A. (editor), Orbital Mechanics: Second Edition, AIAA Inc., New York, NY, 1996.
17. Houbolt, J. C., "Problems and Potentialities of Space Rendezvous", *Astronautica Acta*, Vol. 7, 1961, pp. 406-429.

APPENDICES

Appendix A. Ascent Computer Code

```
{-----}
program MAVCOAST ; {MAV problem with no throttling or aerodynamic
                   constraints}

{-----}
USES SIOUX;
Type  vec = array[1..20] of extended;
      mat = array[1..20,1..20] of extended;

Var
    x,z,w,dw,q,dq  : vec;
    OutputFile : TEXT;

    i,j,ghost      :integer;
    ge,             {gravitational acceleration of the earth}
    Pi,             {Pi r not squared, Pi r round}
    Th,             {thrust generated by the vehicle engines}
    m0,             {initial total mass of the vehicle}
    mdot,           {mass flow rate of engines}
    mprop,          {mass of propellant consumed during ascent}
    rfinal,         {radius at engine cutoff}
    vrfinal,        {radial velocity at engine cutoff}
    vthetafinal,   {tangential velocity at engine cutoff}
    rcirc,          {desired final radius of circular orbit}
    deltav,         {magnitude of circularization burn}
    rcut,           {desired engine cutoff radius}
    oec,            {orbital energy constant}
    vcut,           {path velocity at engine cutoff}
    vrcut,          {radial velocity at engine cutoff}
    vthetacut,     {tangential velocity at engine cutoff}
    phicut,         {angle to local horizontal at engine cutoff}
    KAC,            {Kepler Area Constant}
    eccen,          {eccentricity of the orbit prior to circularization}
    rp,             {perigee radius of orbit prior to circularization}
    a,              {semimajor axis of orbit prior to
                   circularization}

    time,           {time during controlled flight}
    t,              {time during vertically constrained flight}
    H,              {Hamiltonian of the system}
    mpl,            {mass of vehicle payload, samples and crew}
    ms,             {mass of empty spacecraft structure}
    mf,             {mass of fuel}
```

za,	{costate variable for radius}
zb,	{costate variable for radial velocity}
zc,	{costate variable for tangential velocity}
Isp,	{specific impulse}
gmars,	{gravitational acceleration on Mars}
GM,	{gravitational parameter for Mars}
vorbit,	{circular orbit velocity at desired final altitude}
Rm,	{Radius of Martian surface 3310 km}
rstar,	{distance scaling variable}
vstar,	{velocity scaling variable}
tstar,	{time scaling variable}
treal,	{unsclaed time}
vmagsq,	{square of the magnitude of velocity}
phi,	{angle of flight path to local horizontal}
alfa,	{angle of thrust vector to flight path}
accel,	{acceleration of the vehicle, thrust over instantaneous mass}
csphal,	{cosine of alpha}
snphal,	{sine of alpha}
tcon,	{time during controlled flight}
pitch,	{altitude at which controlled flight begins}
numeng,	{number of engines on vehicle}
throttle	{percent of engine thrust}

:extended;

{-----}

Procedure Parameters;

```

begin
SIOUXSettings.tabspaces := 0;
Pi:= 3.141592653589793238462643;
GM:=4.28283e13;           { Grav Parameter of Mars, m3/s2}
mpl:= 1000.0;            {kg mass payload crew and samples}
ms:= 8898.0;             {kg mass structure}
mf:= 39000.0;           {kg of fuel initial}
m0 := mpl+mf+ms;        {46681 kg initial mass of vehicle}
Rm := 3310000.0;        {m, radius of Mars}
numeng:=3.0;
throttle:=1.0;
mdot :=26.46*numeng*throttle; {kg/s}
ge:= 9.81; {m/s}
Isp:= 379.0;             {ISP of Engine}
gmars:= 3.909;          {1g on Mars m/s2}
rstar:=Rm;
vstar:=sqrt(GM/Rm);

```

```

tstar:=sqrt(Rm*Rm*Rm/GM);
pitch:= 3000.0;           {pitchover altitude}
Th := mdot*ge*Isp;       {N}

{please specify}
rcirc:= Rm + 250000.0;    {m}
deltav:= 25.0; {m/s}
rcut:= Rm + 160000.0;    {m}

vorbit:= sqrt(GM/(rcirc)); {desired final velocity}
oec:= ((vorbit-deltav)*(vorbit-deltav)) - (2*GM/rcirc);
KAC:= (vorbit-deltav)*rcirc;
eccen:=sqrt(1.0 + (KAC*KAC*oec/(GM*GM)));
rp:=rcirc*(1.0-eccen)/(1.0+eccen);
a:=(rcirc+rp)/2.0;
vcut:=sqrt(GM/rcut)*sqrt(2.0-(rcut/a));
vthetacut:=rcirc*(vorbit-deltav)/rcut; {rapogee*vapogee/r}
vrcut:= sqrt( vcut*vcut - vthetacut*vthetacut);

```

```
end;
```

```

{-----}
{          NUMERICAL ROUTINES          }
{-----}

```

```
function arctan2(r,s : extended) : extended;
```

```
var q: extended;
```

```
begin
```

```
  if s= 0.0 then
```

```
    if r>0 then q:=Pi/2 else q:=-Pi/2
```

```
  else
```

```
    q:= arctan(r/s);
```

```
  if s<0.0 then
```

```
    if r<0.0 then q:=q-Pi else q:= q+Pi;
```

```
  if r=0.0 then q:= 0.0;
```

```
  arctan2:= q;
```

```
end;
```

```
{-----}
```

```
procedure Runge( procedure de(t:extended; var y,dy:vec); n :integer; h :extended;
```

```
var t :extended; var y :vec );
```

```
var y1,f1,f2,f3,f4 :vec;
```

```
  i : integer;
```

```
  h2 : extended;
```

```
begin
```

```
  h2:= h/2;
```

```

de( t,y,f1 );
for i:=1 to n do y1[i]:= y[i] + h2*f1[i];
t:=t + h2;

de( t,y1,f2 );
for i:=1 to n do y1[i]:= y[i] + h2*f2[i];

de( t,y1,f3 );
for i:=1 to n do y1[i]:= y[i] + h *f3[i];
t:=t + h2;

de( t,y1,f4 );
for i:=1 to n do y[i]:= y[i] + h/6*(f1[i]+2*(f2[i]+f3[i])+f4[i]);
end;
{-----}
Procedure Vecroot( procedure Vector(var x,y :vec); var x,ybase :vec;
                    ndim :integer; delx :extended );
type mat = array[1..20,1..20] of extended;
var    y,x1          :vec;
       jacob         :mat;
       errlast,err,det :extended;
       i,j,k         :integer;

procedure System(n :integer; var a :mat; var b,x :vec; var det :extended);
var    i,j,m: integer;
       k: extended;
begin
    det := 1.0;
    for m := 1 to n-1 do begin
        det := det*a[m,m];
        for i := m+1 to n do begin
            k := a[i,m]/a[m,m];
            for j := m+1 to n do a[i,j] := a[i,j] - k * a[m,j];
            b[i] := b[i] - k*b[m];
        end;
    end;
    det := det * a[n,n];
    for m := n downto 1 do begin
        x[m] := b[m]/a[m,m];
        for i := 1 to m -1 do b[i] := b[i] - x[m]*a[i,m];
    end;
end;

begin

```

```

errlast:= inf;
for k:= 1 to 25 do begin
  Vector( x,ybase );
  err:= 0;
  for i:= 1 to ndim do err:= err + sqr(ybase[i]);
  err:= sqrt(err);
  {writeln('Vecroot : ', err);}
  if (err<10) and (k>3) and (err>=errlast) then exit(Vecroot);
  errlast:= err;

  { Calculate Jacobian }
  for j:= 1 to ndim do begin
    x[j]:= x[j] + delx;
    Vector( x,y );
    for i:= 1 to ndim do jacob[i,j]:= (y[i]-ybase[i]) / delx;
    x[j]:= x[j] - delx
  end;

  { Solve for correction vector and correct x }
  System( ndim,jacob,ybase,x1,det );
  for i:= 1 to ndim do x[i]:= x[i] - x1[i];
end;
{writeln('Solution not found in "Vecroot"')}
end;
{-----}
Procedure Climbeqs (y:extended; var q,dq :vec);
begin

  dq[1] := -mdot*tstar/m0;           {mdot}
  dq[2] := q[4];                     {rdot}
  dq[3] := q[5]/q[2];                {thetadot}
  dq[4] := (q[5]*q[5]/q[2]) + (-1.0/(q[2]*q[2])) + Th/(q[1]*m0*gmars);{vrdot}
  dq[5] := 0.0;                       {vthetadot}

end;
{-----}
Procedure Climb;
begin
  q[1] := 1.0;   {mass0}
  q[2] := 1.0;   {r0}
  q[3] := 0.0;   {theta0}
  q[4] := 0.0;   {vr0}
  q[5] := 0.0;

  t := 0.0;
  repeat

```

```

Runge( Climbeqs, 5, 0.001, t, q );
writeln(t*tstar:10:5,chr(9){,q[1]*m0:10:5,chr(9)},
        (q[2]-1.0)*rstar:10:5,chr(9) ,q[3]:10:5,chr(9),
        q[4]*vstar:10:5,chr(9), q[5]*vstar:10:5,chr(9));

until q[2] > (Rm+pitch)/rstar;
writeln(t:10:5,chr(9),q[1]:10:5,chr(9),q[2]:10:5,chr(9),q[3]:10:5,chr(9),
        q[4]:10:5, chr(9),q[5]:10:5,chr(9));
end;
{-----}
Procedure Equations( y:extended; var w,dw :vec );

begin

vmagsq:= (w[5]*w[5]) + (w[4]*w[4]);           {magnitude velocity squared}
phi:= arctan2(w[4],w[5]);                     {angle to local horizon}
alfa:= arctan2(w[7],w[8])-phi;                 {control law}
csphal:= cos(alfa + phi);
snphal:= sin(alfa + phi);
accel:= Th/(w[1]*m0*gmars);                    {F/m*go}

dw[1] := -mdot*tstar/m0;                       {mdot}
dw[2] := w[4]; {rdot}
dw[3] := w[5]/w[2]; {thetadot}
dw[4] := (w[5]*w[5]/w[2]) - 1.0/(w[2]*w[2]) + accel*snphal; {vrdot}
dw[5] := (-w[4]*w[5]/w[2]) + accel*csphal; {vthetadot}
dw[6] := w[7]*( (w[5]*w[5]/(w[2]*w[2])) - (2.0/(w[2]*w[2]*w[2])) ) +
        w[8]*( -w[4]*w[5]/(w[2]*w[2]) ); {z1dot}
dw[7] := -w[6] + w[7]*(-accel*csphal*w[5]/vmagsq) + w[8]*( (w[5]/w[2]) +
        (accel*snphal*w[5]/vmagsq) ); {z2dot}
dw[8] := w[7]*( (-2.0*w[5]/w[2]) + accel*csphal*w[4]/vmagsq) +
        w[8]*( (w[4]/w[2]) - (accel*snphal*w[4]/vmagsq) ); {z3dot}

end;
{-----}
Procedure Solve;
Var a0,a1,a2,a3,a4,a5,b0,b1,b2,b3,b4,b5,Dr,Di,xi,theta,D: extended;
begin

w[1] := q[1]; {mass0}
w[2] := q[2]; {r0}
w[3] := q[3]; {Theta0}
w[4] := q[4]; {vr0}
w[5] := q[5]; {vtheta0}
w[6] := x[1];

```

```

w[7] := x[2];
w[8] := x[3];
      {put in init conditions}
tcon := t;

repeat
  Runge( Equations, 8, 0.001, tcon, w );

until tcon > time;

vmagsq:= (w[5]*w[5]) + (w[4]*w[4]);      {magnitude velocity squared}
phi:= arctan2(w[4],w[5]);                {angle to local horizon}
alfa:= arctan2(w[7],w[8])-phi;           {control law}

csphal:= cos(alfa + phi);
snphal:= sin(alfa + phi);
accel:= Th/(w[1]*m0*gmars);              {F/m*go}
H:= -1.0 + w[6]*(w[4]) + w[7]*((w[5]*w[5]/w[2]) - 1.0/(w[2]*w[2]) +
  accel*snphal ) + w[8]*((-w[4]*w[5]/w[2]) + accel*csphal );

end;
{-----}
procedure Vecset( var x,z :vec);
begin
  Solve;
  z[1]:= H;
  z[2]:= w[2]*rstar - (rcut);
  z[3]:= w[4]*vstar- vrcut;

end;
{-----}
Procedure Search;
begin
  x[1] := 0.5;      {guess conditions of costate vector}
  x[2] := 0.5;
  x[3] := 0.5;

  Vecroot(Vecset, x,z,3,1e-5);

end;
{----- MAIN -----}

begin

Parameters;

```



```

Climb;
time:=430.0/tstar; {t}
Repeat
  Search;
  treal:=tcon*tstar;
  mprop := m0*(w[1]);
  rfinal := (w[2]*rstar)-3310000.0;
  vrfinal := w[4]*vstar;
  vthetafinal := w[5]*vstar;
  za:= x[1];
  zb:= x[2];
  zc:= x[3];

  phicut:=arctan2(vrcut,vthetacut);
  vmagsq:= (w[5]*w[5]) + (w[4]*w[4]);
  phi:= arctan2(w[4],w[5]);           {angle to local horizon}
  alfa:= arctan2(w[7],w[8])-phi;     {control law}

  csphal:= cos(alfa + phi);
  snphal:= sin(alfa + phi);
  accel:= 293576.61/(w[1]*m0*gmars);           {F/m*go}
  H:= -1.0 + w[6]*(w[4]) + w[7]*((w[5]*w[5]/w[2]) - 1.0/(w[2]*w[2]) +
  accel*snphal ) + w[8]*((-w[4]*w[5]/w[2]) + accel*csphal );

  writeln( rp-3310000.0:15:5, chr(9), vcut:15:10, chr(9), rcut-3310000.0:15:10,
  chr(9), vrcut:15:10,chr(9), vthetacut:15:10, chr(9), H:15:5,chr(9), phicut:15:10,
  chr(9));

  writeln( treal:15:5, chr(9), (w[1]*m0)-(ms+mpl):15:10, chr(9), rfinal:15:10,
  chr(9), vrfinal:15:10, chr(9), vthetafinal:15:10, chr(9), H:15:5, chr(9), phi:15:10,
  chr(9), accel:15:10, chr(9));

  writeln( za:15:5,chr(9),zb:15:10,chr(9),zc:15:10,chr(9));

  time := time + 0.001;
until time >491.3/tstar;      {at 491.3 the guage reads E on 3 engines}
                              {at 368.4 the guage reads E on 4 engines}

end.

```

Appendix B. Rendezvous Code

```
{-----}
program HILL ; {Rendezvous Problem with target in elliptical orbit,
               chaser in circular orbit}
{-----}
USES SIOUX;
Type  vec = array[1..20] of extended;
      mat = array[1..20,1..20] of extended;

Var
    x,z,w,dw : vec;
    OutputFile : TEXT;

    i,j,ghost : integer;
    fx,        {initial x force in ERV coordinate system}
    fy,        {initial y force in ERV coordinate system}
    fz,        {initial z force in ERV coordinate system}
    a,         {semimajor axis of ERV orbit}
    e,         {eccentricity of ERV orbit}
    incl,      {relative inclination between ERV and MAV orbit}
    nuE,       {ERV initial true anomaly}
    nudotE,   {ERV initial true anomaly time rate of change}
    nudotM,   {MAV initial true anomaly time rate of change}
    nuM,       {MAV initial true anomaly}
    xEPC,     {ERV x coordinate in Planetocentric coordinate
              system}
    yEPC,     {ERV y coordinate in Planetocentric coordinate
              system}
    zEPC,     {ERV z coordinate in Planetocentric coordinate
              system}
    xMPC,     {MRV x coordinate in Planetocentric coordinate
              system}
    yMPC,     {MRV y coordinate in Planetocentric coordinate
              system}
    zMPC,     {MRV z coordinate in Planetocentric coordinate
              system}
    rERV,     {ERV initial radius}
    rMAV,     {MAV initial radius}
    rp,       {Perimars Radius of ERV}
    rE,       {initial radius of ERV}
    rM,       {initial radius of MAV}
    vp,       {Perimars velocity of ERV}
    x0PC,     {initial x distance in Planetocentric coordinate system}
    y0PC,     {initial y distance in Planetocentric coordinate system}
```

zOPC,	{initial z distance in Planetocentric coordinate system}
x0,	{initial x distance in ERV coordinate system}
y0,	{initial y distance in ERV coordinate system}
z0,	{initial z distance in ERV coordinate system}
rho0,	{magnitude of inital distance}
xdot0,	{initial x relative velocity in ERV coordinate system}
ydot0,	{initial y relative velocity in ERV coordinate system}
zdot0,	{initial z relative velocity in ERV coordinate system}
thetaE,	{path angle of ERV}
vE,	{ERV inital velocity}
vEx,	{ERV initial x velocity in ERV coordinates}
vEy,	{ERV initial y velocity in ERV coordinates}
vEz,	{ERV initial z velocity in ERV coordinates}
vM,	{MAV circular orbit velocity}
vMxPC,	{MAV initial x velocity in Planetocentric coordinates}
vMyPC,	{MAV initial y velocity in Planetocentric coordinates}
vMzPC,	{MAV initial z velocity in Planetocentric coordinates}
vMxEC,	{MAV initial x velocity in ERV coordinates}
vMyEC,	{MAV initial y velocity in ERV coordinates}
vMzEC,	{MAV initial z velocity in ERV coordinates}
relvelx,	{Relative x velocity in ERV coordinates}
relvely,	{Relative y velocity in ERV coordinates}
relvelz,	{Relative z velocity in ERV coordinates}
DelVx1,	{Delta V x for first manuever}
DelVy1,	{Delta V y for first manuever}
DelVz1,	{Delta V z for first manuever}
delV1,	{Magnitude of delta V for first manuever}
DelVx2,	{Delta V x for second manuever}
DelVy2,	{Delta V y for second manuever}
DelVz2,	{Delta V z for second manuever}
delV2,	{Magnitude of delta V for second manuever}
GM,	{Gravitational Parameter of Mars}
Time,	{time rate which solution is calculated}
Pi,	{Pie are round}
t,	{time in R-K interation}
nudoubledot,	{time varying angular acceleration}
rT	{time varying ERV radius}
:extended;	

{-----}

Procedure Parameters;

```
begin
  SIOUXSettings.tabspace := 0;
  Pi := 3.141592653589793238462643;
```

GM := 4.28283e4; {Gravitational Parameter (Mars), km³/s²}

{ERV orbital characteristics}

e := 0.8249022;
rp := 3560.0; {km}
nuE := 1.0*Pi/180.0; {radians}
a:=rp/abs(e-1); {km}
vp:=sqrt(GM*(1+e)/rp); {km/s}

{MAV circular orbit characteristics}

incl:= 0.0*Pi/180.0; {radians}
nuM:=0.0*Pi/180.0; {radians}
rM:=3560.0; {km}
vM:=sqrt(GM/rM); {km/s}
nudotM:=sqrt(GM/rM)/rM; {radians/sec}

{Calculation of relative distances}

rE:=rp*(1.0+e)/(1+(e*cos(nuE)));
nudotE:=vp*rp/(rE*rE); {rads/sec}
xEPC:=rE*cos(nuE); {km}
yEPC:=rE*sin(nuE); {km}
zEPC:=0.0; {km}
xMPC:=rM*cos(incl)*cos(nuM); {km}
yMPC:=rM*cos(incl)*sin(nuM); {km}
zMPC:=rM*sin(incl); {km}

{Relative Distance in ERV coordinate system}

x0 := (xMPC-xEPC)*sin(nuE) - (yMPC-yEPC)*cos(nuE); {km}
y0 := (yMPC-yEPC)*sin(nuE) + (xMPC-xEPC)*cos(nuE); {km}
z0 := zMPC-zEPC; {km}
rho0:=sqrt((x0*x0)+(y0*y0)+(z0*z0)); {km}
fx := 0.0;
fy := 0.0; {N}
fz := 0.0;

end;

{-----}
{ NUMERICAL ROUTINES }
{-----}

function arctan2(r,s : extended) : extended;

var q: extended;
begin
if s= 0.0 then

```

        if r>0 then q:=Pi/2 else q:=-Pi/2
    else
        q:= arctan(r/s);
    if s<0.0 then
        if r<0.0 then q:=q-Pi else q:= q+Pi;
    if r=0.0 then q:= 0.0;
    arctan2:= q;
end;
}-----}
procedure Vecroot( procedure Vector(var x,y :vec); var x,ybase :vec;
                    ndim :integer; delx :extended );
type mat = array[1..20,1..20] of extended;
var    y,x1                :vec;
        jacob              :mat;
        errlast,err,det    :extended;
        i,j,k              :integer;

procedure System(n :integer; var a :mat; var b,x :vec; var det :extended);
var    i,j,m: integer;
        k: extended;
begin
    det := 1.0;
    for m := 1 to n-1 do begin
        det := det*a[m,m];
        for i := m+1 to n do begin
            k := a[i,m]/a[m,m];
            for j := m+1 to n do a[i,j] := a[i,j] - k * a[m,j];
            b[i] := b[i] - k*b[m];
        end;
    end;
    det := det * a[n,n];
    for m := n downto 1 do begin
        x[m] := b[m]/a[m,m];
        for i := 1 to m -1 do b[i] := b[i] - x[m]*a[i,m];
    end;
end;

begin
    errlast:= inf;
    for k:= 1 to 25 do begin
        Vector( x,ybase );
        err:= 0;
        for i:= 1 to ndim do err:= err + sqr(ybase[i]);
        err:= sqrt(err);
        {writeln('Vecroot : ', err);}
    end;
end;

```

```

    if (err<10) and (k>3) and (err>=errlast) then exit(Vecroot);
    errlast:= err;

    { Calculate Jacobian }
    for j:= 1 to ndim do begin
        x[j]:= x[j] + delx;
        Vector( x,y );
        for i:= 1 to ndim do jacob[i,j]:= (y[i]-ybase[i]) / delx;
        x[j]:= x[j] - delx
    end;

    { Solve for correction vector and correct x }
    System( ndim,jacob,ybase,x1,det );
    for i:= 1 to ndim do x[i]:= x[i] - x1[i];
end;
writeln("Solution not found in "Vecroot")
end;
{-----}

```

```

procedure Runge( procedure de(t:extended; var y,dy:vec); n :integer; h :extended;
                var t :extended; var y :vec );
var    y1,f1,f2,f3,f4 :vec;
        i : integer;
        h2 : extended;
begin
    h2:= h/2;

    de( t,y,f1 );
    for i:=1 to n do y1[i]:= y[i] + h2*f1[i];
    t:=t + h2;

    de( t,y1,f2 );
    for i:=1 to n do y1[i]:= y[i] + h2*f2[i];

    de( t,y1,f3 );
    for i:=1 to n do y1[i]:= y[i] + h *f3[i];
    t:=t + h2;

    de( t,y1,f4 );
    for i:=1 to n do y[i]:= y[i] + h/6*(f1[i]+2*(f2[i]+f3[i])+f4[i]);
end;
{-----}

```

```

Procedure Equations( y:extended; var w,dw :vec );

```

```

begin
rT:= rp*(1+e)/(1+(e*cos(w[7])));
nudoubledot:= -2.0*Gm*e*sin(w[7])/(rT*rT*rT);

dw[1] := w[2];
dw[2] := fx - GM*w[1]/(rT*rT*rT) + 2*w[8]*w[4] + nudoubledot*w[3]
      +w[8]*w[8]*w[1];
dw[3] := w[4];
dw[4] := fy + 2*GM*w[3]/(rT*rT*rT) - 2*w[8]*w[2] + nudoubledot*w[1] +
      w[8]*w[8]*w[3];
dw[5] := w[6];
dw[6] := fz - GM*w[5]/(rT*rT*rT);
dw[7] := w[8];
dw[8] := -2.0*Gm*e*sin(w[7])/(rT*rT*rT);

{ writeln(dw[1]:20:10,dw[2]:20:10);}

end;

```

```

{-----}
Procedure Solve;
Var a0,a1,a2,a3,a4,a5,b0,b1,b2,b3,b4,b5,Dr,Di,xi,theta,D: extended;
begin
{ writeln('PARAM:',a0:10:5,b0:10:5,a1:10:5,b1:10:5,a2:10:5,b2:10:5,
a3:10:5,b3:10:5,a4:10:5,b4:10:5,Dr:10:5,Di:10:5,D:10:5);}

```

```

w[1] := x0;
w[2] := x[1];
w[3] := y0;
w[4] := x[2];
w[5] := z0;
w[6] := x[3];
w[7] := nuE;
w[8] := 0.00131733;
t := 0.0;
repeat
  Runge( Equations, 8, 0.1, t, w );
  If Ghost = 1 then

```

```

writeln(t:10:5,chr(9),w[1]:15:10,chr(9),w[2]:15:10,chr(9),w[3]:16:10,chr(9),w[4]:
15:10,chr(9), w[5]:15:10,chr(9),w[6]:15:10);

```

```

until t > Time*60.0;

```

```

end;
{-----}
procedure Vecset( var x,z :vec);
  begin
    Solve;

    z[1]:= w[1];
    z[2]:= w[3];
    z[3]:= w[5];

  end;

{-----}
Procedure Search;
  begin

    x[1] := 0.0;
    x[2] := -0.0;
    x[3] := 0.0;

    Vecroot(Vecset, x,z,3,1e-5);

  end;

{----- MAIN -----}

begin

Parameters;

writeln( Time:10:8,chr(3),x0:15:10,chr(9),y0:15:10,chr(9),z0:15:10,chr(9),rho0:15:10);

Time := 1.0;
  Repeat
    Parameters;
    Search;
    xdot0 := x[1]; ydot0 := x[2]; zdot0 := x[3];

    {CALCULATION OF INITAL ACTUAL RELATIVE VELOCITIES}
    thetaE:=arctan2(e*sin(nuE),(1+(e*cos(nuE))));
    vE:=vp*rp/(rE*cos(thetaE));
    vEx:=-vE*cos(thetaE);
    vEy:=vE*sin(thetaE);
    vEz:=0.0;
    vMxPC:=(-nudotM*sin(incl)*zMPC) - (nudotM*cos(incl)*yMPC);
    vMyPC:=nudotM*cos(incl)*xMPC;
  
```



```

vMzPC:=nudotM*sin(incl)*xMPC;
vMxEC:=vMxPC*sin(nuE)-vMyPC*cos(nuE);
vMyEC:=vMxPC*cos(nuE)+vMyPC*sin(nuE);
vMzEC:=vMzPC;
relvelx:=vMxEC - vEx + nudotE*y0;
relvely:=vMyEC - vEy - nudotE*x0;
relvelz:=vMzEC - vEz;
DelVx1:=xdot0-relvelx;
DelVy1:=ydot0-relvely;
DelVz1:=zdot0-relvelz;
delV1:=sqrt((DelVx1*DelVx1)+(DelVy1*DelVy1)+(DelVz1+DelVz1));
DelVx2:=w[2];
DelVy2:=w[4];
DelVz2:=w[6];
delV2:=sqrt((w[2]*w[2])+(w[4]*w[4])+(w[6]*w[6]));

```

```
writeln(Time:10:8,chr(3),xMPC:15:10,chr(9),yMPC:15:10,chr(9),zMPC:15:10,chr(9));}
```

```
writeln(Time:10:8,chr(3),DelVx1:15:10,chr(9),DelVy1:15:10,chr(9),{DelVz1:15:10,chr(9),}delV1:15:10,DelVx2:15:10,chr(9),DelVy2:15:10,chr(9),{DelVz2:15:10,chr(9),}delV2:15:10);
```

```

Time := Time + 1.0;
until Time > 120.0;

```

```
end.
```

VITA

Stephen Edward Stasko was born on May 31, 1976 in Portsmouth, Virginia, the son of Edward and Marie Stasko. Soon after his birth his family moved to Philadelphia, Pennsylvania, where he received his early education in the Catholic school system, graduating from Archbishop Ryan High School in June of 1994. He entered Drexel University in September of 1994, where, as a cooperative student, he held several jobs in the course of his undergraduate education, both in the university as a teaching assistant and in the VIZ Corporation as a design engineer. In June of 1999 he graduated Magna Cum Laude from Drexel with a Bachelor of Science in mechanical engineering. Shortly afterwards, in August of 1999, he began to pursue a Masters Degree in Aerospace Engineering at the University of Tennessee Space Institute under Dr. Gary Flandro. His research area included orbital mechanics and trajectory optimization.